THE DISTRIBUTION OF COMPTON SCATTERED ANNIHILATION PHOTONS, AND THE EINSTEIN-PODOLSKY-ROSEN ARGUMENT

Leonard Ralph Kasday

Submitted in partial fulfillment of the requirements
for the degree of Doctor of Philosophy
in the Faculty of Pure Science
Columbia University

1972

TABLE OF CONTENTS

Jeff 6-28-83

ABSTRACT

The relative polarization of the two photons emitted when a positron annihilates at rest has been re-investigated with high precision and a different method of data analysis. An experiment using a pair of ideal polarization analyzers to measure this relative polarization would be a special case of the general class of thought experiments discussed by Einstein, Podolsky, and Rosen (EPR). EPR argued from these thought experiments that a physical system can exist in a state with definite values for two non-commuting variables. Since quantum mechanics can not describe such a state, EPR called quantum mechanics "incomplete". But EPR believed a complete theory---sometimes called a hidden variable theory--is possible. (This argument of EPR is sometimes called the Einstein-Podolsky-Rosen "paradox".)

Our experimental results, together with a theorem due to Bell, provide strong evidence that a local "hidden variable" theory is not possible. The results also rule out a hypothetical modification of quantum mechanics, suggested by Bohm and Aharonov, which was motivated by the EPR thought experiments.

Compton scattering was used to analyze the linear polarization. But the theorem of Bell, mentioned above, applies to relatively "ideal" polarization measurements. Therefore, it was necessary to prove the existence, and find the explicit form of the function f relating Compton and ideal linear polarization measurements. The existence of f is shown here to follow from general principles of quantum mechanics, plus parity and angular momentum conservation; the explicit form of f is deduced from the Klein-Nishina equation. Experimental evidence is cited against the argument that f may be different in a local "hidden variable" theory.

ACKNOWLEDGMENTS

I would like to express sincere appreciation of Professor C. S. Wu for suggesting this research and for her invaluable encouragement and advice. I would also like to thank Dr. Jack Ullman, my collaborator on this experiment, for all his contributions to the design work and analysis that appears below. Discussions with J. M. Jauch, J. S. Bell, and especiallly R. Friedberg were very helpful. Professor Jauch brought the work of Langhoff to my attention; Professor Friedberg greatly clarified the significance of Bell's theorem. The criticism of G. Feinberg, H. Goldstein, and S. Lang were most constructive. Thanks are also due to all the staff of Pegram Laboratories, for their conscientiousness and the continually high quality of their work; to Barbara Stanley for typing the preliminary copy of the manuscript, and Patricia Grange for typing the final copy of the manuscript.

Chapter I

Introduction and Summary

A. Historical Introduction

Quantum mechanics had enjoyed well known success as a framework for describing a multitude of physical phenomena. Nevertheless, some physicists believe that in its present form quantum mechanics is only an approximation to a more complete physical theory; among these physicists was Albert Einstein.

It was Einstein's belief that in the more complete physical theory, contrary to the usual interpretation of quantum mechanics, physical variables would have definite values before they were measured. He offered philosophical arguments for this belief, and in turn was answered by philosophical arguments.

Then in 1957, Bohm and Aharonov (Bo 57,60) pointed out the significance of a practical experiment which had in fact already been performed. Wu and Shaknov (Wu 50) had in 1950 measured the relative linear polarization of the photons emitted upon positron annihilation in a metal. Bohm and Aharonov showed that this experiment ruled out a certain hypothetical modification of quantum mechanics which was motivated by some of Einstein's ideas.

But it was J. S. Bell (Be 64, 70) who, in 1964, showed that a suitable experiment would rule out Einstein's complete theories--if the experimental results agreed with the quantum predictions. It is shown in this chapter that, if certain reasonable assumptions are permitted, then a more extensive version of the Wu-Shaknov measurement is a suitable experiment.

Before Bell's work was published, the Wu-Shaknov experiment had been already repeated by Bertolini et al. (Be 55) and Langhoff (La 60). Wu and Shaknov had analyzed the linear polarizations by Compton scattering in aluminum. Langhoff used scatterers made of plastic scintillators to help discriminate against background events, used detectors subtending scattering angles much smaller than Wu and Shaknov's, and in addition made measurements at many different azimuthal Compton scattering angles. The results of all three experiments agreed with quantum predictions. However, certain data needed for the analysis presented below, which shows how Bell's theorem can be applied, was not recorded (viz., n_1 and n_2 in Equation 14).

The Wu-Shaknov experiment has again been repeated (Ka 70a, 70b). All necessary data was recorded. Also, in the present experiment data were taken simultaneously over different scattering angles--with the actual scattering angles for each event determined by the energy of the scattered photons.

The results of this experiment are in excellent agreement with the quantum predictions. This constitutes strong evidence against the possibility of the complete theories envisaged by Einstein (referred to as local hidden variable theories by Bell). It must be born in mind that the evidence is strong but not absolute, since additional assumptions have been introduced. The experiment also confirms that the Bohm-Aharonov hypothesis may be ruled out.

B. A Summary of the Quantum Predictions for Polarization Measurements Made on Annihilation Photons.

It follows* (Ya 50) from conservation of parity and angular momentum that when a positron and electron which are both at rest annihilate into two photons, the angular momentum and parity J^P of the photon state is

$$J^P = 0^-$$

and therefore the state may be represented by the vector

$$\Psi = \frac{|RR\rangle - |LL\rangle}{\sqrt{2}} \qquad (1a)$$

where $|RR\rangle$($|LL\rangle$) is a state containing two right (left) circularly polarized protons with momenta along the Z axis. This may also be written

$$\Psi = \frac{|XY\rangle - |YX\rangle}{\sqrt{2}} \qquad (1b)$$

where $|XY\rangle$ is the state containing a photon moving in the +Z direction with linear polarization along the X axis and a photon moving in the -Z direction with polarization along the Y axis. $|YX\rangle$ is a similar state.

The implications of Equations 1a and 1b are as follows:

1. Suppose the linear polarization of either photon is measured. The probability that the result will be X is 1/2, and the probability that the result will be Y is 1/2.

2. Suppose simultaneous linear polarization measurements are made on the two photons. Whenever the result X is obtained for one, the result Y will be obtained for the other; and whenever the result Y is obtained for one, the result X will be obtained for the other.

3. When circular polarization measurements are made on either photon,

---

*See Appendices A and B for physical and formal derivations.

the probability of obtaining L is 1/2 and the probability of obtaining R is 1/2.

4. Suppose simultaneous circular polarization measurements are made on the two photons. Whenever the result R is obtained for one, the result R will also be obtained for the other; whenever the result L is obtained for one, the result L will also be obtained for the other.

C. The Einstein Podolsky Rosen Argument.

In his autobiography, Einstein described* his conception of an individual physical system, on which a measurement was about to be performed:

> (i) The individual system (before the measurement) has a definite value. . .for all variables of the system, and more specifically that value which is determined by a measurement of this variable. Proceeding from this conception. . . . The Ψ-function is no exhaustive description of the real situation of the system but an incomplete description; it expresses only what we know on the basis of former measurements concerning the system.

He contrasted it with the following conception, held by a hypothetical believer in the completeness of quantum mechanics.

> (ii) The individual system (before the measurement) has no definite value of [the variables]. . . . The value of the measurement only arises in cooperation with the unique probability which is given to it in view of the Ψ-function only through the act of measurement itself. Proceeding from this conception, he will (or, at least, he may state: the Ψ-function is an exhaustive description of the real situation of the system. . . .

Einstein believed that if conception (i) is true, then

> The statistical character of the present theory [quantum mechanics] would then have to be a necessary consequence of the incompleteness of the description of the systems in quantum mechanics, and there would no longer exist any ground for the supposition that a future basis of physics must be based upon statistics.

Some years earlier, in 1935, Einstein, Podolsky and Rosen (EPR) had presented (Ei 35) an argument supporting Einstein's conception, (i) above. Their argument is now presented in terms of the two annihilation photons discussed in the preceding sections of this chapter. (EPR actually considered a whole class of wavefunctions of a pair of parti-

---

*The original and the English translation may be found in (Ei 49).

cles; the two photons provide an example of that class.)

Let the photons be labeled 1 and 2. Suppose the photons are separated by a large distance. Let CP(1) = the circular polarization of photon 1, let LP(1) = the linear polarization of photon 1, etc.

1. After CP(1) is measured, the result of a measurement of CP(2) can be immediately predicted.
2. Therefore, immediately after the measurement is performed on photon 1, photon 2 has a definite CP.

Now, the crucial hypothesis of locality is used:

3. However, because 1 and 2 were separated by a large distance, the measurement on 1 could not disturb 2 instantaneously.
4. Statement 3 implies that before 1 was measured, 2 must have had a definite CP. That is, 2 must have a definite CP <u>whether 1 is measured or not</u>. This is an assumption.

1'. Similarly, LP(1) <u>could</u> have been measured.

2' and 3'. (These are analogous to 2 and 3 above.)

4'. B must have a definite LP <u>whether 2 is measured or not</u>.

Thus, according to EPR, before any measurement, the photons have both definite CP and definite LP; and EPR held that quantum mechanics is incomplete in that it cannot describe* a state having definite CP and LP. This conclusion is precisely the content of Einstein's conception (i) of a physical system. [It is necessary to speak of CP and LP as "variables" which can have two possible "values" in order to explicitly match the conclusion to (i).] Furthermore, EPR believed, though they did not

---

*because a state of definite LP is a superposition of two states of opposite CP.

prove, that a "complete" theory, which would specify in advance the result of all measurements on the photons, could be found.

D. An Experimental Test of Einstein's Conception: Bell's Inequality

It might seem that it is solely a philosophical question whether a physical quantity has a definite value before it is measured. However, J. S. Bell (Be 64, 70) has shown that the answer to the question can be verified by experiment---at least in principle. For concreteness, Bell's result will now be described in terms of the two-photon system described above. The discussion actually applies to any pair of widely separated systems.

Bell's contribution was to show that Einstein's contention leads to restrictions of the results of measurements. Consider then the 2 photon system. According to Einstein's conception, the result M_i of a measurement on a physical quantity is equal to the value that quantity possessed just before the measurement:

$$M_i = \lambda_i \text{ at time just before measurement}$$

where λ_i = the value of the physical quantity.

Bell hypothesized a more general measurement which contains Einstein's as a special case: first, the result M of the measurement may depend on more than one of the physical quantities associated with the system; also, M may depend on the setting m of a "knob" on the instrument making the measurement. This may be written

$$M = M(\underline{\lambda}, m) \qquad (2)$$

where $\underline{\lambda}$ = the set of values $\{\lambda_i\}$ of the physical quantities associated with the system. Note that $\underline{\lambda}$ and m are hypothesized to determine the exact value of M with certainty. In contrast, quantum mechanics only predicts probability relations between the state of the system and the output of a measuring instrument.

Bell, like Einstein, made the important hypothesis of locality. Like Einstein, he hypothesized that M could not depend on physical operations made a large distance away.

The name "local hidden variables" may be given to the set λ, because of the locality hypothesis and because if such variables exist, they are "hidden" from present day knowledge and measurements.

Now consider a particular type of measurement, made on photons by an instrument with an adjustable knob and a single numerical output. (For example, the instrument may contain a linear polarization filter, and produce a +1 or -1 output according to whether the photon passes through the filter or not. The knob on the instrument determines the angle which the filter makes with some axis.)

Consider the following experiment: Let two of the instruments just described be placed some large distance apart, and let a source S of annihilation photons be placed between them.

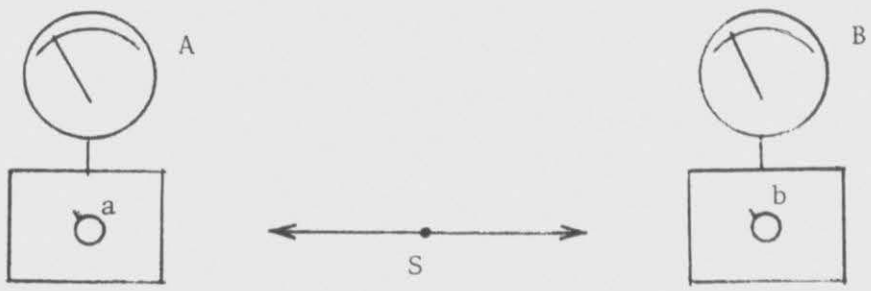

The instrument on the left performs measurements on the photons moving toward the left. Let its output be denoted by the quantity A, and its knob setting by a. Similarly, the instrument on the right has output B and knob position b.

Bell showed that the "hidden variable" hypothesis, Equation (2), and the locality hypothesis [described just after Equation (2)] lead to an inequality on the results of the measurements. Furthermore, the quantum

predictions for certain special cases of this experiment violate the inequality. Hence, if experimental test verifies the quantum predictions, one or both of those hypotheses must be false.

Bell's inequality may be stated as follows: First, write

$$\begin{aligned} A &= A(a,\underline{\lambda}) \\ B &= B(b,\underline{\lambda}) \end{aligned} \tag{3}$$

symbolizing the dependence of the instrument outputs A, B, on $\underline{\lambda}$ and their knob settings a and b. Note that since locality requires that A not depend on the physical operation of turning the knob on the other, distant, instrument, A has no dependence on b. Similarly B does not depend on a.

Imagine the photons to be emitted a large number N_o of times. Define the probability ρ distribution by*

$$\rho(\underline{\lambda}) = N(\underline{\lambda})/N_o \tag{4}$$

where $N(\underline{\lambda})$ is the number of times the physical variables have the values collectively denoted by $\underline{\lambda}$.

Define P(a,b) as the average of A·B taken over many emissions; it depends of course on the knob positions a, b, and is clearly given by

$$P(a,b) \equiv \overline{A \cdot B} = \sum_{\underline{\lambda}} \rho(\lambda)\ A(a,\underline{\lambda})\ B(b,\underline{\lambda}) \tag{5}$$

For mathematical convenience assume

$$\begin{aligned} -1 \leq A(a,\lambda) \leq 1 \\ -1 \leq B(b,\lambda) \leq 1 \end{aligned} \tag{6}$$

No generality is lost by this assumption; for the meter scale on any instrument can always be relabeled to satisfy this requirement. Let a, b, c, d be <u>any</u> 4 knob settings. Bell showed very simply that Equations

---

*Changes in the notation for continuous variables will be omitted here.

(5) and (6) lead to the following inequality on P(ab) (Be 70):

$$|P(db) + P(dc)| + |P(ab) - P(ac)| \leq 2 \qquad (7)$$

where a, b, c, and d are any four possible knob settings.

The theorem is easily generalized to include an extra set of hidden variables which influence the reading of instrument A, and a set influencing B, provided each set not depend on the setting of the other instrument. If these additional hidden variables are inserted in Equation (5) an equation of the same form as (5) results with A and B replaced by $\overline{A}$ and $\overline{B}$, which are defined as averages of A and B with respect to the extra hidden variables:

$$P(ab) = \sum_{\underline{\lambda}} \rho(\underline{\lambda})\ \overline{A}(a,\underline{\lambda})\ \overline{B}(b,\underline{\lambda}) \qquad (8)$$

The inequality (7) remains valid.

It is important to remember that Bell's inequality is a direct restriction on the outputs of the measuring instruments, rather than on the physical variables the instruments measure. This implies that an experiment designed to test Bell's inequality might be interpreted differently than the usual physics experiment.

The usual physics experiment is designed to test some theoretical relation between various physical variables like momentum, spin, or polarization, for example. The experimenter does not see these variables directly, of course. Instead, he sees the outputs of his measuring instruments, and uses the relation between those outputs and the physical variables, to find the physical variables. The relation he uses is generally established by strong evidence accumulated over many years, so he can be very sure the relation is correct. But strictly speaking, he can never be absolutely positive it is correct; he assumes it is correct. He rarely if ever explicitly states the assumption though. In other words,

the usual physics experiment involves implicit assumptions which are usually not stated.

In contrast, Bell's inequality does not refer to physical variables; instead it refers directly to the outputs of the measuring instruments. This raises the possibility that the inequality can be tested without assuming (implicitly or explicitly) that the relations between the instrumental outputs and the physical variables are correct (as must be done in the usual physics experiments). This possibility would be realized with a hypothetical "ideal" polarization detector. An ideal polarization detector, by definition,* has the following outputs:

+1 for photons polarized parallel to the detector axis

-1 for photons polarized perpendicular to the detector axis

cos 2ϕ, for photons with polarizations making an angle ϕ with detector axis

Now suppose we place a source of annihilation photons between two such detectors. Define the quantities A and B in Equation (3) as the outputs of the two detectors, and a and b as the angles the detectors' axes make with the horizontal plane, then a simple quantum mechanical calculation yields:

$$P(ab) = -\cos 2(a-b) \qquad (9)$$

If we substitute

---

*The existence of an ideal detector is consistent with the laws of quantum mechanics, because the first two parts of the definition are clearly consistant, and the third part of the definition (the cos 2ϕ dependence) may be derived from the first two parts of the definition.

$$2a = 0°,\ 2b = 135°,\ 2c = 45°,\ 2d = 90°$$

into Bell's inequality, Equation (7), we obtain

$$2\sqrt{2} \leq 2$$

The inequality is violated. Therefore if the quantum predictions are correct, a hidden variable theory would be ruled out.

Now suppose this ideal experiment could be performed. Quantum mechanics is needed to <u>design</u> the experiment. However, no quantum mechanics is needed to interpret the results! This is because (as already stated) Bell's inequality applies directly to the outputs of the instruments; i.e., to the "meter readings" A and B. Hence if the meter readings violate Bell's inequality, then local hidden variable theories are ruled out immediately, without relating the meter readings to any underlying physical variables; and therefore without assuming that the quantum relations used to design the experiment are correct.

Unfortunately, this intriguing possibility cannot be realized in practice. For no ideal polarization detectors* have yet been found for annihilation photons [nor the optical photons involved in an analogous experiment discussed by Horne (Ho 69) and Clauser et al. (Cl 69).] Consider, for example, Compton polarimeters. The output of a Compton polarization measurement is either "a photon was scattered into the gamma detector" or "the photon was not scattered into the gamma detector". In order to apply Bell's inequality <u>directly</u> to the polarimeter outputs, it is necessary to assign numerical values to the possible outputs. For example, the output A of one detector might be defined as +1 (-1)

---

*Actually an ideal analyzer need not exist. There could in principle exist an "almost ideal analyzer" which would not be perfectly efficient but would produce outputs which would violate Bell's inequality. But no one has found such an "almost ideal" analyzer either.

when the scattered photon hits (does not hit) the gamma detector; and the output B of the other detector can be similarly defined. Also, the quantities a,b in P(a,b) can be taken as the angular placements of the gamma detectors.

But when this is done, it turns out that the P(ab) that results does not violate Bell's inequality. Hence, for these definitions of A and B, a direct application of Bell's inequality to the instrumental outputs can not rule out local hidden variable theories (cf. Cl 69).

One might think that some other definitions of A and B, or some clever arrangement of many gamma detectors could circumvent this difficulty. But this is not the case, for, as shall now be shown, it is possible to construct an ad-hoc local hidden variable theory that reproduces all the results of Compton scattering of annihilation photons. Therefore, no direct analysis of Compton scattering could possibly violate Bell's inequality.

The two counter examples which show that Compton scattering experiments can not provide absolute proof against hidden variable theories may be described as follows:

1. Bell (private communication) has produced a counter-example, described in Appendix C, in which the correlation between the scattering events at the two detectors arises from their dependence on a single hidden variable. The model reproduces the quantum predictions for all momentum measurements that could be made on the two scattered photons. So clearly no function of momentum measurements, including any P(ab), could ever violate Bell's inequality. Hence, no such Compton scattering experiment can absolutely rule out a local hidden variable theory. Bell's counter-example does not apply when the photons have energies somewhat lower

than the masses of the particles which scatter them. For this reason Bell suggests that it might be useful to perform the experiment on photons of different energy. It should be noted though that another counter-example, simpler if perhaps more artificial than Bell's, is not subject to this restriction on the photon energy.

2. The other counter-example may be described as follows: let the hidden parameters be vectors $\hat{\lambda}_1$, $\hat{\lambda}_2$ associated with particles and let the photons ultimately scatter in the directions of these vectors. Then simply give $\hat{\lambda}_1$, $\hat{\lambda}_2$ the same probability distribution as that of the momenta $\hat{k}_1$, $\hat{k}_2$ of the scattered photons

$$\rho(\hat{\lambda}_1\hat{\lambda}_2) = F(\hat{\lambda}_1\hat{\lambda}_2) \ , \tag{10}$$

where

$F(\hat{k}_1\hat{k}_2)$ = the probability distribution of the directions of the scattered photons.

In other words, one may picture the photons as having "decided in advance," at the time of annihilation, in which directions they would ultimately scatter. The model is clearly local; for example, changing the position of detector 1 does not affect the parameter $\hat{\lambda}_2$. It should be clear that the model reproduces the results of <u>all</u> measurements that can be made on the scattered photons. Thus it is seen again that* a Compton scattering experiment can not absolutely rule out a local hidden variables theory.

The reason a similar model cannot reproduce quantum predictions for the ideal measurements is that setting the ideal analyzers to several different angles corresponds to measuring several <u>non-commuting observables</u>. Quantum theory does not supply a <u>joint</u> probability distribution function like $F(\hat{k}_1\hat{k}_2)$ for non-commuting observables, so the model cannot be constructed as above.

---

*This would be so even if the experimental results did not agree with quantum theory, for then F could simply be set equal to the experimental results.

E. Assumptions Needed to Apply Bell's Inequality to Compton Scattering

Even though a Compton experiment cannot rule out hidden variable theories, it can provide strong evidence against them. The following assumptions shall be made:

1. It is possible in principle to construct an ideal linear polarization analyzer.
2. The results obtained in an experiment using ideal analyzers and the results obtained in a Compton scattering experiment are correctly related by quantum theory.

Assumption 2 may be clarified as follows: Suppose 1 or more photons Compton scatter. It is shown in Chapter II, below, that according to quantum theory, the angular distribution of the scattered photons can be computed from the results which would have been obtained in an ideal polarization analysis of the photons and vice-versa. The computation involves only the Compton scattering results and the ideal polarization results. No specification of the photon state is necessary. Assumption 2 is that this relation between the ideal measurement results and the Compton results is correct.

This relation is possible because when the photons' polarizations are resolved into components parallel and perpendicular to the scattering planes, interference effects between the components vanish when the Compton scattering is computed. This was pointed out by Snyder et al. (Sn 48). The interference terms vanish because Compton scattering is not sensitive to the sense of circular polarization. See Chapter II. (Snyder et al. used a different argument. The experimental evidence for the validity of the theory of Compton scattering is discussed in Appendix E.

With the aid of assumptions 1 and 2, Bell's inequality for ideal polarization analyzers was used to calculate corresponding restrictions on the angular distribution of Compton scattered photons. The result will be given below in Equations 16-18.

F. The Bohm Aharonov Hypothesis.

Considerations of the EPR situation have led Bohm and Aharonov (BA) (Bo 57, 60) to consider the hypothesis that quantum theory breaks down in a particular way for widely separated particles. An argument motivating the hypothesis is given below. Also, Jauch (Ja 70) has shown how considerations involving the notion of a state in axiomatic quantum theory can also motivate the BA hypothesis.

It is shown in Appendix D that any theory obeying the BA hypothesis can be put in the mathematical form of a local hidden variable theory.

The hypothesis may be motivated as follows: consider again the two annihilation photons 1 and 2. After a CP measurement on 1, photon 2 will be either in the state

$$|R\rangle = \frac{|X\rangle + i|Y\rangle}{\sqrt{2}} \tag{11}$$

or in the state

$$|L\rangle = \frac{|X\rangle - i|Y\rangle}{\sqrt{2}} \tag{12}$$

Thus, after the measurement on 1, CP(2) is definite and known [viz., the same as the result of the CP(1) measurement]. However, photon 2 is in a superposition of states of different LP, so LP(2) can not be considered definite---nor even definite but unknown---because interference effects between the states of different LP could be detected. But if LP(1) [instead of CP(1)] had been measured, then LP(2) would have been definite, while CP(2) could not have been considered definite---nor even definite but unknown. In other words, the "status" of LP(2) and CP(2), i.e., which one may and which one may not be considered to have a definite

value, can be instantly fixed by means of a distant measurement: a measurement which could not have involved any physical interactions with photon 2 (assuming no interaction can travel with infinite speed). Of course, this does not at all mean that any observational change in photon 2 was caused by the measurement on 1. Nevertheless, the change in "status" of the variables CP(2) and LP(2) by means of the measurement on 1 seems somewhat peculiar, and BA sought to avoid this peculiarity.*

Thus, Bohm and Aharonov examined the following hypothesis: that quantum theory is valid for particles which are close together, but that after the photons are some "large distance" apart their state vector Ψ changes into a product of state vectors for the individual photons.** Then a measurement on photon 1 would affect the state vector of 1 but not the state vector of 2, and therefore the status of LP and CP of 2 would no longer be changed by the measurement on 1. Jauch (private communication) has remarked that in the case of positron annihilation the "large distance" involved might be much larger than the coherence length (~7 cm) of the annihilation process.

Bohm and Aharonov hypothesized further that the state vector would not always change into the same product state, but rather it would change at random into one member of an ensemble of product states. This ensemble would possess rotational symmetry around the Z axis and reflection symmetry in the XY plane so that the average of many measurements would exhibit the expected rotational and reflective symmetries. In other words, the pure state would change into a symmetric mixture. But

---

*BA termed the situation "paradoxical."

**More precisely, the creation operator of the state becomes the product of a creation operator for a photon with momentum in the +Z direction, and a creation operator for a photon with momentum in the -Z direction.

according to the Schrodinger equation a pure state must change into a pure state.

Thus the BA hypothesis implies a new law governing the time behavior of the two particles.

BA showed that it is impossible in practice to rule out the BA hypothesis by means of position and momentum measurements on the annihilation photons [or on the particles involved in any scattering experiment]. However, the hypothesis can be tested by measuring the linear polarizations of the annihilation photons. A direct calculation (outlined in Appendix D) shows that all mixtures obeying the BA hypothesis (with rotational and reflective symmetry) lead to a P(ab) of the form*

$$P(ab) = C \cos 2(a-b) \qquad (13)$$

$$\text{with} \quad |C| \leq 1/2.$$

Quantum theory, on the other hand, violates this inequality by predicting C = -1, so quantum theory and the BA hypothesis can be distinguished experimentally. Of course, if the linear polarization is measured by Compton scattering, it is necessary to assume that the quantum predictions are valid for the Compton scattering process before determining if the BA hypothesis is valid. Evidence for the validity of quantum predictions for Compton scattering is discussed in Appendix E.

---

*This form of the result is simpler than that given by Bohm and Aharonov. A similar computation has also been performed by Jauch (Ja 70).

G. Description of the Experiment Performed and the Definition of R.

The experimental arrangement is shown in Figures 1 and 2. Positrons were emitted by a radioactive source, stopped and annihilated (in copper) at 0 (Figure 1). The annihilation gamma rays were emitted in all directions; the vertical direction was selected by a lead collimator which is omitted in Figure 1 but is drawn in Figure 2. Events were sought in which the annihilation photons Compton scattered on electrons in S_1 and S_2, and entered detectors D_1 and D_2 which measured their energies. Lead slits positioned at angles ϕ_1 and ϕ_2 selected the range of azimuthal angles Φ_1 and Φ_2 which were accepted. The top slit-detector assembly was rotated to vary the relative azimuthal angle.

Background (false) events were virtually eliminated by making the scatterers S_1 and S_2 out of plastic scintillators: we required a 4-fold time coincidence among the two scatterers and the two detectors (S_1, S_2, D_1, D_2) and also imposed a "sum energy requirement" that the total energy deposited in each scatterer plus detector equal the energy of an annihilation photons.

The sensitivity of a Compton analyzer to polarization depends mainly on three factors:

Factor A. The spread of azimuthal angles Φ_1, Φ_2 selected by the lead slits. (See Figure 1a.)

Factor B. The probability for a photon to scatter more than once in the scatterer.

Factor C. The effective efficiencies of the detectors as a function of scattered photon energy.*

---

*Since the energy of the scattered photon is a function of the polar Compton scattering angle, the "effective" energy efficiency depends on the geometry of the apparatus.

These factors were taken into account as follows: The scatterer diameters were made small so that the spread of azimuthal angles accepted was well defined, and the effect of the spread could be accurately determined. The small diameters also minimized the probability of photons scattering more than once in the scatterer. To compute the efficiencies of the detectors as a function of scattered photon energy, we compared the measured energy spectrum with the theoretical energy spectrum, allowing for finite detector resolution; then we computed the effect of the efficiencies, again allowing for detector resolution. (In the actual computations the numerical values of the efficiencies never appeared explicitly.)

The data were analyzed by computing for each value of the relative azimuthal angle $(\phi_2 - \phi_1)$ the quantity R defined by

$$R(\phi_1\phi_2) = \left. \frac{N/N_{ss}}{n_1/N_{ss}\ n_2/N_{ss}} \right|_{\phi_1\phi_2} \qquad (14)$$

were

N_{ss} = [number of times the two photons Compton scatter].

N = [number of times the two photons Compton scatter] and both photons are detected.

n_1 = [number of times the two photons Compton scatter] and only photon 1 is detected.

n_2 = [number of times the two photons Compton scatter] and only photon 2 is detected.

ϕ_1,ϕ_2 = the azimuthal angles at which the lead slits are positioned (to be distinguished from Φ_1,Φ_2 which refer to the photons).

For comparison of our results with theory the quantity R has a number of useful properties:

1. If the momenta of the scattered photons were uncorrelated, R would equal 1. Deviations of R from 1 correspond to correlations between the momenta.

2. A number of instrumental effects cancel out of the expression for R; for example, source strength and slit width (to first order).
3. Quantum theory predicts a simple relation between R and the quantity P(ab) associated with the ideal polarization analyzers which were described in the paragraph preceding Equation (9):

$$R(\phi_1\phi_2) = 1 - B_{QTh} P(\phi_1\phi_2) \tag{15}$$

where B_{QTh} is an instrumental factors depending mainly on factor A, factor B, and factor C mentioned above. Equation 15 is derived and discussed in Chapter III. It is emphasized that this relation is valid for <u>any</u> polarization state of the two photons and hence for any P(ab). For the particular case of the two photons emitted in positron annihilation, Equations (9) and (15) yield

$$R(\phi_1\phi_2) = A - B \cos 2(\phi_2 - \phi_1), \tag{16}$$

with

$$\begin{aligned} A &= 1 \\ B &= B_{QTh} \end{aligned} \tag{17}$$

(In addition, the 180° correlation between the annihilation photons can change the value of A by ~ 0.05 and B by ~0.02 because of geometrical effects.)

If experiment shows that R is given by Equation (16) with A = 1, then reference to Equation (15) shows that $P(\phi_1\phi_2)$ is proportional to $\cos 2(\phi_2 - \phi_1)$; and it is easily seen that

$$\begin{aligned} &B = B_{QTh} \text{ if quantum theory is valid} \\ &B \leq B_{QTh}/\sqrt{2} \text{ if a local hidden variable theory is valid} \\ &B \leq B_{QTh}/2 \text{ if the Bohm-Aharonov hypothesis is valid.} \end{aligned} \tag{18}$$

The data were divided into "energy regions" defined as follows: Let e_1, e_2 be the outputs of the detectors which measure the energies of

the scattered photons. (Since the detectors have finite resolution, the relation between e_1, say, and the energy of scattered photon 1 is not one to one.) We computed R, including in N, n_1, and n_2 only those events falling in specified regions in the e_1,e_2 plane (shown in Figure 3). Also, the "whole" region was defined as containing events of all e_1e_2. When R is calculated over the whole region, the statistical uncertainties are small, but a numerical integration of the polarization correlation over a wide range of scattered photon energies is necessary. This gives a "washing out" of the correlation and leaves our results open to the objection that perhaps the correlation was really smaller than predicted by theory, but the numerical integration was in error. Also, there are large systematic uncertainties in B when R is calculated for the whole region. The values of R for the small regions in ℓ_1 and ℓ_2 depend only slightly on the details of numerical integration and can be much more accurately computed.

H. Results and Conclusions

Figure 4 shows R for the "whole" region as a function of relative azimuthal angle $(\phi_2-\phi_1)$. The points are fit well by a curve of the form of Equation (16) with A = 1.007 ± 0.004. The ±0.004 represents statistical uncertainty. This value of A is influenced by certain geometrical effects, and from this value we deduce that the value that would have been obtained with ideal geometry is 1.01 ± 0.05, which is consistent with 1. Thus in the subsequent analysis the validity of Equation (16) with A = 1 could be assumed, and the values of B were compared with the expressions in Equation (18). The comparison is plotted in Figure 5. The theoretical predictions are corrected for instrumental effects. Error bars are given for systematic uncertainties in these instrumental corrections and for statistical uncertainties in the experimental points. The particularly large uncertainty in the theoretical values for B for the "whole" region is due to the presence of events in which a scattered photon did not deposit its full energy in the detector. The theoretical values of B could be more accurately determined in regions 1, 2, 3, and 4, which contained fewer of these events. In each case, the experimental value of B agreed with the quantum prediction and exceeded the upper limits derived from Bell's inequality and from the BA hypothesis.

The following conclusions were drawn:

1. We find no evidence for a breakdown in the quantum predictions for Compton scattering of annihilation protons. Our results, therefore, are consistent with the work of Wu and Shaknov (Wu 50), who were the first to show good quantitative agreement between quantum theory and experiment; the work of Bertolini et al. (Be 55), and the excellent, thorough work of Langhoff (La 60). [Also H. Muller (Mu 64) has verified the

quantum predictions for circular polarization.]

2. Furthermore, if we make the assumption that it is possible in principle to construct an ideal linear polarization analyzer and that quantum theory correctly relates results obtained with ideal and Compton analyzers, then it follows that a local hidden variable theory cannot describe the annihilation photons. However, if the introduced assumptions were not valid then counter-examples described in section 2a above show that this type of experiment cannot rule out local hidden variable theories.

3. Finally, assuming that the quantum theory of Compton scattering is correct, we conclude that the Bohm Aharonov hypothesis does not hold for this experimental arrangement.*

---

*Jauch suggested however, that the BA hypothesis may still be valid when the photons are separated by much more than twice the coherence length, when the flight paths of the photons are unequal, or when two different particles are involved. Twice the coherence length is about 14 cm; the photons were separated by ~25 cm before scattering in this experiment and by ~50 cm in Langhoff's (La 60).

Chapter II

The Relation Between Ideal Polarimeter Results and Compton Polarimeter Results

Linear polarization measurements can be made on a photon with either (1) an "ideal" polarization analyzer, in principle or (2) a Compton polarimeter.

An ideal polarization analyzer is defined to produce a unique output, viz. +1 (-1), upon measuring a photon with linear polarization parallel (perpendicular) to the analyzer axis. In contrast, a Compton polarimeter does not give a unique output for any particular polarization state of the photons. Instead, such a polarimeter Compton scatters the photon, and the polarization of the incoming photon determines the probability that the scattered photon will be found with various directions of momentum.

There exists a function f relating ideal and Compton polarization measurements. The existence of f shall now be shown to follow from general principles of quantum mechanics, plus parity and angular momentum conservation; the explicit form of f shall be deduced from the Klein-Nishina equation.

A. The existence of the relation

Consider a photon which Compton scatters off an electron which is initially at rest. The initial state Ψ_1 of the electron-photon system is given by

$$\Psi_1 = |i\rangle [q|X\rangle + r|Y\rangle] \tag{1}$$

where

$|i\rangle$ = an electron with zero linear momentum and spin state i

$|X\rangle$, $|Y\rangle$ = a photon with momentum along the z axis and linear polarization in the x,y direction

q,r = numbers, complex in general, normalized so that

$$q\,q + r\,r = 1 \tag{2}$$

The final state Ψ_2 of the system is given by

$$\Psi_2 = |jk\rangle \tag{3}$$

where

k = the momentum of the scattered photon

j = the polarizations of the recoil electron and scattered photon. These are the variables which will be summed over to find the final result.

Also let

E, Θ, Φ = the energy, polar scattering angle, and azimuthal scattering angle of the scattered photon.

The probability dF_k for finding a scattered photon with momentum k is given by

$$dF_k(qr) = \rho(E)\,\frac{1}{2}\sum_i \sum_j |\langle\Psi_2|S|\Psi_1\rangle|^2\, dE\,d\Phi\,d\Theta \tag{4}$$

where

$\rho(E)$ = the density of final states

S = the scattering matrix

$\frac{1}{2}\sum_i$ = the average over initial electron spin states

Substituting for Ψ_1 and Ψ_2 from Equations (1) and (3) we obtain

$$dF_k(qr) = \rho(E)\,\frac{1}{2}\sum_{ij} |\langle jk|S|(q|X\rangle + r|Y\rangle)|i\rangle|^2\, dEd\Phi \qquad (5)$$

The differential $d\Theta$ does not appear in Equation (5) because energy and momentum conservation relates Θ to E. Equation (5) may be expanded as:

$$\begin{aligned} dF_k(qr) = \frac{1}{2}\rho(E)\sum_{ij} \{ & qq^*|\langle jk|S|Xi\rangle|^2 \\ & + rr^*\,|\langle jk|S|Yi\rangle|^2 \\ & + qr^*\langle jk|S|Xi\rangle\langle jk|S|Yi\rangle^* \\ & + rq^*\langle jk|S|Yi\rangle\langle jk|S|Xi\rangle^*\} dEd\Phi \end{aligned} \qquad (6)$$

which is of the form

$$dF_k = [\alpha|q|^2 + \beta|r|^2 + 2\,\mathrm{Re}(\gamma qr^*)]\, dEd\Phi \qquad (7)$$

with α and β real (and positive). γ is complex in general. However, we shall now show that, because of conservation of parity and angular momentum, γ is real.

Now, the electromagnetic interaction is invariant under rotation and parity transformation. Therefore, (since the electrons are not polarized) the scattering probability must be the same for right and left hand circularly polarized photons. Since

$q,r = 1, i$ for right circular polarization, and

$q,r = 1, -i$ for left circular polarization

we have

$$dF_k(1,i) = dF_k(1,-i) \qquad (8)$$

Substituting Equation (8) into Equation (7) yields

$$\alpha + \beta + 2\mathrm{Re}(\gamma i) = \alpha + \beta + 2\mathrm{Re}(\gamma[-i])$$

or

$$2\mathrm{Re}(i\gamma) = 0$$

Hence γ is real and may be taken outside of the "Re" in Equation (7) to yield:

$$dF_k = [\alpha|q|^2 + \beta|r|^2 + 2\,\mathrm{Re}(qr^*)]\,dEd\Phi \tag{9}$$

or

$$\frac{dF_k}{dEd\Phi} = [q^*r^*]\begin{bmatrix}\alpha & \gamma \\ \gamma & \beta\end{bmatrix}\begin{bmatrix}q \\ r\end{bmatrix} \tag{10}$$

Now rotate the x and y axes along which polarization is measured, through an angle ξ about the z axis. Call the new axes x' and y'. The quantities q' and r' are related to q and r by

$$\begin{bmatrix}q' \\ r'\end{bmatrix} = \begin{bmatrix}\cos\xi & -\sin\xi \\ \sin\xi & \cos\xi\end{bmatrix}\begin{bmatrix}q \\ r\end{bmatrix}.$$

Since the matrix in Equation (10) is real, it follows that there exists a ξ such that dF_k is <u>diagonal</u> in q' and r'. Calling the elements of the diagonal matrix α' and β', we have

$$dF_k(qr) = (\alpha'|q'|^2 + \beta'|r'|^2)dEd\Phi \equiv dF_k'(q'r') \tag{11}$$

Note that we have introduced and defined the quantity $dF_k'(q'r')$.

Since dF_k' depends only on $|q'|^2$ and $|r'|^2$, dF_k' can be related to measurements made with the ideal analyzer defined above. An "ideal analyzer" gives an output L' = +1 [-1] for photons polarized along [or perpendicular to] the analyzer axis. Now let the ideal analyzer axis be oriented parallel to the x' axis, which was defined just under Equation (10). Then clearly the mean value of L' for a photon with polarization components q' and r' is

$$\overline{L'}(q'r') = |q'|^2\,(+1) + |r'|^2\,(-1) \tag{12}$$

But Equation (11) may be written

$$dF_k'(q'r') = \frac{1}{2}[(\alpha'+\beta')(|q'|^2+|r'|^2)+(\alpha'-\beta')(|q'|^2-|r'|^2]dEd\Phi$$

Using Equations (12) and (3) this becomes

$$dF'_k(q'r') = \frac{1}{2}\left[\alpha'+\beta' + (\alpha'-\beta')\bar{L}'\right]dEd\Phi \qquad (13)$$

This proves what we set out to show: that there exists a function relating F'_k (the probability of a photon Compton scattering in the direction k) and $\bar{L}'$ (the average output of an ideal analyzer oriented along the x' axis.)

B. That x' must be parallel or perpendicular to the scattering plane.

The following thought experiment is designed to show that x' must be perpendicular or parallel to the scattering plane (the scattering plane is defined as the plane containing the momentum of the scattered photon, k, and the momentum of the incident photon). Imagine a Compton polarimeter consisting of a scatterer, and a detector positioned to detect scattered photons with momentum k. Suppose a beam of photons linearly polarized in direction ε_1 is directed at the polarimeter in the z direction (perpendicular to the paper).

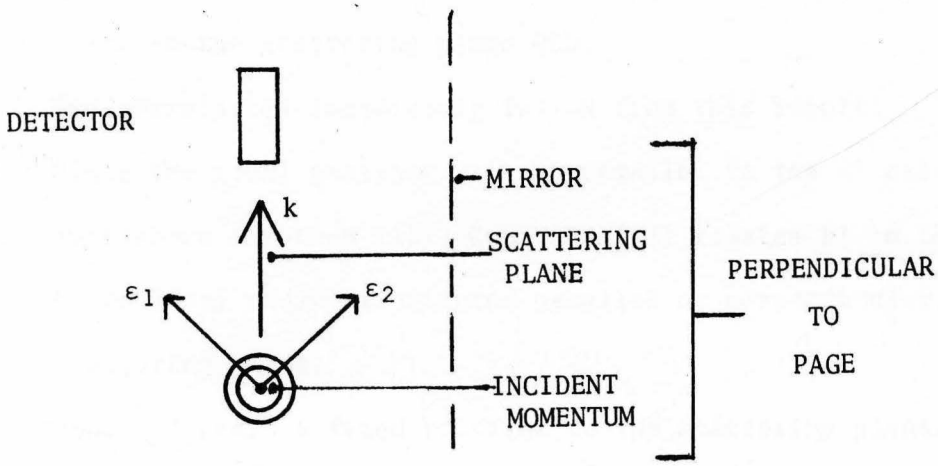

There will be a certain count rate C_1 in the detector. Now imagine a mirror parallel to the scattering plane. By parity conservation, and rotational invariance, a beam of photons with polarization ε_2, the mirror image of the original polarization ε_1, will produce a count rate $C_2 = C_1$. But the count rate is proportional to dF'_k. Using the normalization condition, Equation (2), [$|q'|^2 + |r'|^2 = 1$] Equation (11) becomes

$$dF'_k(q'r') = [1 + (\alpha'-\beta')|q'|^2]dEd\Phi \qquad (14)$$

Therefore, letting q'_1 and q'_2 be the x components of q_1 and q_2, the equality $C_1 = C_2$ implies that

$$q'_1 = q'_2 \qquad (15)$$

The following diagram illustrates that if x' is $\begin{matrix}\text{parallel}\\ \text{perpendicular}\end{matrix}$ to the scattering plane, then $q_2 = \pm q_1$, and Equation (15) is satisfied. Clearly, this

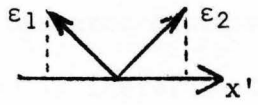

x' perpendicular to scattering plane $[q_2 = -q_1]$

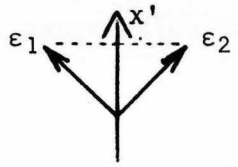

x' parallel to scattering plane $[q_2 = +q_1]$

is the only way Equation (15) can be satisfied, so x' is parallel or perpendicular to the scattering plane QED.

Two corrolaries immediately follow from this result:

1. Since the ideal analyzer axis is parallel to the x' axis, [see just above Equation (12)] Equation (13) relates F_k' to the output of an ideal analyzer oriented parallel or perpendicular to the scattering plane.
2. Since x' bears a fixed relation to the scattering plane, α' and β' in Equation (13) depend only on E; they are independent of Φ. Hence we can rewrite (13) as follows:

$$dF_k'(q'r') = f(E)\ [1 + m(E)\ \overline{L'(q'r')}]\ dE d\Phi \qquad (16)$$

The definitions of f(E) and m(E) can be read off by comparing (6) and (8):

$$f(E) = \frac{1}{2}\ (\alpha' + \beta')$$

$$m(E) = 2\ (\alpha' - \beta')/(\alpha' + \beta')$$

C. The relation between Compton and ideal polarization analysis of multi-photon systems.

In order to proceed, it is necessary to rewrite Equation (16) as an operator equation. Now, F_k' is the average value of the observable $\underset{\sim}{F_k'}$, and is therefore the expectation value of an operator. Similarly, $\bar{L}'$ is the expectation value of an operator $\underset{\sim}{L}'$

$$\begin{aligned} F_k' &= \langle \underset{\sim}{F_k'} \rangle \\ \bar{L}' &= \langle \underset{\sim}{L}' \rangle \end{aligned} \tag{17}$$

where $\langle\rangle$ denotes an expectation value. Equation (16) relates the expectation values of these operators. This relation holds for all q' and r', and hence for all vectors in the Hilbert space. Therefore, the operators themselves satisfy the same relation

$$d\underset{\sim}{F_k} = f(E)\ [1 + m(E)\ \underset{\sim}{L}']\ dE d\Phi/2\pi \tag{18}$$

This operator equation, Equation (18), can be used to compute the relation between Compton and ideal polarization analyzers when more than one photon is involved. For example, consider a polarization analysis of annihilation photons (Figure 1). The probability $dF(k_1 k_2)$ of finding the photons scattered in directions k_1 and k_2 respectively is

$$\begin{aligned} dF(k_1 k_2) = \langle \underset{\sim}{F_{k_1}'}\ \underset{\sim}{F_{k_2}'} \rangle &= f(E_1) f(E_2)\ [1 + m(E_1)\langle \underset{\sim}{L_1'} \rangle + \\ &+ m(E_2)\langle \underset{\sim}{L_2'} \rangle + m(E_1) m(E_2) \langle \underset{\sim}{L_1'} \underset{\sim}{L_2'} \rangle]\, dE_1 dE_2 d\Phi_1 d\Phi_2 / 4\pi^2 \end{aligned} \tag{19}$$

where $\underset{\sim}{L_1'}$ and $\underset{\sim}{L_2'}$ refer to ideal polarization measurements of photons 1 and 2 respectively.

By rotational symmetry about the z axis, $\langle \underset{\sim}{L_1'} \rangle = \langle \underset{\sim}{L_2'} \rangle = 0$. Furthermore, since $\langle \underset{\sim}{L_1'} \underset{\sim}{L_2'} \rangle$ is the average product of the outputs of two hypothetical measuring instruments, we can call it $P(\Phi_1 \Phi_2)$, the symbol introduced just before Equation (12) of Chapter 1:

$$p(\Phi_1\Phi_2) = \langle L_1' L_2' \rangle \tag{20}$$

where Φ_1, Φ_2 are the angles the axes of the ideal analyzers make with the X-Y plane. Then Equation (19) becomes

$$dF(k_1'k_2') = f(E_1)f(E_2)[1+m(E_1)m(E_2)P(\Phi_1\Phi_2)]dE_1dE_2d\Phi_1d\Phi_2/4\pi^2 \tag{21a}$$

This then is the relation between Compton and ideal polarimeter measurements on a pair of annihilation photons.

Furthermore, according to quantum mechanics, $P(\Phi_1\Phi_2)$ is given by

$$P(\Phi_1\Phi_2) = -\cos 2(\Phi_2-\Phi_1) \tag{21b}$$

D. The explicit form of the relation.

The Klein-Nishina cross section (Kl 29) for a linearly polarized photon, summed over the possible polarization states of the scattered electron and scattered photon (Ev 58), may be written in the following form:

$$d\sigma(E_o,E,\Phi) = \frac{r_o^2}{2} \frac{m_e c^2}{E_o^2} \chi(E_o,E) \left[1 - \frac{\sin^2\Theta}{\chi(E_o E)} \cos 2\Phi\right] dE d\Phi \quad (22)$$

where

E_o = the energy of the incident photon

E = the energy of the scattered photon

Φ = the angle between the incident photon polarization and the scattering plane

r_o = the classical electron radius 2.82×10^{-13} cm

$m_e c^2$ = the electron rest mass energy

Θ = the scattering angle, related to E by

$$e c^2 (1/E + 1/E_o) = 1 - \cos\Theta$$

and

$$\chi(E_o E) = E_o/E + E/E_o - \sin^2\Theta$$

From Equation (12) the average response of an ideal polarization analyzer to a linearly polarized photon is

$$L = \cos 2\Phi \quad (23)$$

where Φ = the angle between the photon polarization and the analyzer axis. Inserting (23) into (16) and comparing with (22), it is seen that

$$f(E) = \frac{r_o^2}{2} \frac{m_e c^2}{E_o^2} \chi(E_o E)$$

$$m(E) = -\sin^2 H / \chi(E_o E) \quad (24)$$

The function m(E) is plotted in Figure 15 for $E_o = m_e c^2$.

Chapter III

DESIGN OF THE EXPERIMENT

The bracketed factor, $[1 + m(E_1)m(E_2)P(\Phi_1\Phi_2)]$ in Equation 21 of Chapter II expresses the polarization correlation between the scattered photons. The data was analyzed to produce the quantity R, defined above in section G of Chapter I, which, assuming the validity of quantum mechanics, is just that factor in the first approximation.

A. First approximation to R

During each experimental run,

1. The lead slits that defined the azimuthal angles Φ_1, Φ_2 of the scattered photons were in fixed positions ϕ_1, ϕ_2. The widths of the slit openings, $\Delta\phi_1$, $\Delta\phi_2$ were constant throughout all the runs.
2. The outputs of the NaI detectors, e_1', e_2' were recorded for each event satisfying the "N", "n_1", or "n_2" requirements defined in Equation 14 of Chapter I and in Figure 1.*

During and after the runs, the events were sorted to yield the numbers

$N(e_1\Delta e_1\ e_2\Delta e_2\ \phi_1\Delta\phi_1\ \phi_2\Delta\phi_2)$ ≡ number of "N" events (see Equation 14 Chapter I) with:

$$e_1 \le e_1' \le e_1 + \Delta e_1 \qquad (1a)$$
$$e_2 \le e_2' \le e_2 + \Delta e_2$$

$n_1(e_1\Delta e_1\ \phi_1\Delta\phi_1)$ = number of "n_1" events satisfying

$$e_1 \le e_1' \le e_1 + \Delta e_1 \qquad (1b)$$

---

*The relation of e_1' and e_2' to the actual energies E_1 and E_2 of the scattered photons was complicated by the finite resolution of the detector and the escape of photons that Compton scattered and escaped from the NaI instead of falling in the full energy peak.

$$n_2(e_2 \Delta e_2 \ \phi_2 \Delta \phi_2) = \text{etc.} \qquad (1c)$$

R has already been defined (Equation 14 of Chapter I) as

$$R = \frac{\frac{N}{N_{ss}}}{\frac{n_1}{N_{ss}} \cdot \frac{n_2}{N_{ss}}} \qquad (2)$$

where N_{ss} = the number of scatterer-scatterer coincidences.

Five approximations were made :

Approximation 1.

The annihilation photons emerge from a point source and the diameter of the scatterers is negligible.

Suppose the source is placed at the origin and the scatterers are placed on the +Z axis, as shown in Figure 7. Let

Z_1, Z_2 = Z coordinates of points where photons scatter

E_1, E_2 = energies of scattered photons

Φ_1, Φ_2 = azimuthal angles of scattered photons;

note that these are all upper case symbols and refer to the scattered photons. The lower case symbols e_1, Δe_1, ϕ_1. . .previously defined are parameters of the experimental apparatus.

Strictly speaking, a photon state cannot have definite Z, E, and Φ, because the energy and Z-position operators do not commute. However, for purposes of computing effects associated with the gross dimensions of the apparatus, we made

Approximation 2

The commutator of the energy and Z-position operators is 0, and one can label the photon states by ($ZE\Phi$).

One can, in principle, determine which particular values of ($ZE\Phi$) of the scattered photon were realized by means of suitable measurements

on the recoil electron; hence photon states of different E, Z, Φ will not interfere and a description in terms of probabilities, rather than probability amplitudes, is possible.

Define:

$\mu(Z_1Z_2)$ = conditional probability that the photons scattered at Z_1,Z_2 given they both did indeed scatter;

μ is normalized so

$$\int\int \mu \, dZ_1 \, dZ_2 = 1$$

According to Equations 21a,b of Chapter II the probability F that the scattered photons have energies E_1, E_2 and azimuthal angles Φ_1, Φ_2 is given by

$$\begin{aligned} F(E_1E_2\Phi_1\Phi_2) &\equiv dF(k_1k_2)/dE_1dE_2d\Phi_1d\Phi_2 \\ &= f(E_1)f(E_2)[1-m(E_1)m(E_2)\cos 2(\Phi_2-\Phi_1)]/4\pi^2 \end{aligned} \tag{3}$$

After the photons scatter they may enter the detectors.

Approximation 3

Neglect the polarization sensitivity of the NaI detectors (See Appendix F, item 7, to see how a small polarization dependence arises).

Now let

$g_1(Z_1E_1\Phi_1)$ = the probability that a photon with Z_1, E_1, Φ_1 is detected by detector D_1, set at ϕ_1, and the output e_1 of the detector falls between e_1 and $e_1+\Delta e_1$.

where the subscript 1 on g_1 is an abbreviation for $(e_1 \, \Delta e_1 \, \phi_1 \, \Delta\phi_1)$.

With these definitions, the numbers N_{12}, n_1, n_2 in Equations (1) and (2) are given by

$$\begin{aligned} N &= N_{ss}\int g_1(Z_1E_1\Phi_1)\; g_2(Z_2E_2\Phi_2)\; F(E_1E_2\Phi_1\Phi_2)\; \mu(Z_1Z_2)\; dZ_1dZ_2dE_1dE_2d\Phi_1d\Phi_2 \\ n_1 &= N_{ss}\int g_1(Z_1E_1\Phi_1)\; F(E_1E_2\Phi_1\Phi_2)\; \mu(Z_1Z_2)\; dZ_1dZ_2dE_1dE_2d\Phi_1d\Phi_2 \\ n_2 &= \text{the expression for } n_1 \text{ with } 1 \rightleftarrows 2. \end{aligned} \tag{4}$$

Approximation 4

$$\mu(Z_1Z_2) = \mu_1(Z_1)\mu_2(Z_2) \tag{5}$$

This is discussed in section B.1.a. below. Let

$$G_1(E_1\Phi_1) = \int g_1(Z_1E_1\Phi_1)\mu_1(Z_1)dZ_1 \tag{6a}$$

Approximation 5

Approximate G by a product of a E-function and a Φ-function:

$$G_1(E_1\Phi_1) = G^{e_1\Delta e_1}(E_1)G^{\Delta\phi_1}(|\Phi_1-\phi_1|) \tag{6b}$$

with

$$G^{\Delta\phi_1}(\Phi) = G^{\Delta\phi_1}(-\Phi) \tag{6c}$$

Using Equations (1) through (6) one finds that R in Equation 2 is equal to the "correlation term" in square brackets[ ] in Equation (3),except that $m(E_1)$ and $m(E_2)$ are replaced by certain weighted averages and the cosine dependence is attenuated by the finite slit widths $\Delta\phi_1\Delta\phi_2$:

$$R = 1 - \bar{m}_1\bar{m}_2\,(1-\varepsilon_\phi)\,\cos 2(\phi_2-\phi_1) \tag{7a}$$

or, more explicitly

$$R = 1 - \bar{m}_1(e_1\Delta e_1)\bar{m}_2(e_2\Delta e_2)[1-\varepsilon_\phi(\Delta\phi_1\Delta\phi_2)]\cos 2(\phi_2-\phi_1) \tag{7b}$$

where

$$\bar{m}_1(e_1\Delta e_1) = \frac{\int G_1{}^{e_1\Delta e_1}(E_1)f(E_1)m(E_1)dE_1}{\int G_1{}^{e_1\Delta e_1}(E_1)f(E_1)dE_1} \tag{7c}$$

$$\bar{m}_2(e_2\Delta e_2) = \text{same expression as } \bar{m}_1 \text{ except } 1 \to 2. \tag{7d}$$

$$1-\varepsilon_\phi(\Delta\phi_1\Delta\phi_2) = \frac{\int G^{\Delta\phi_1}(\Phi_1)G^{\Delta\phi_2}(\Phi_2)\cos 2(\Phi_2-\Phi_1)d\Phi_2d\Phi_1}{\int G^{\Delta\phi_1}(\Phi_1)G^{\Delta\phi_2}(\Phi_2)d\Phi_2d\Phi_1} \tag{7e}$$

Our method for evaluating these expressions is contained in sections B.1.c. and B.2. below.

B. Corrections to R

1. Geometric corrections

a. X, Y, Z correlations (ε_μ)

When the first approximation to R was derived in Section A, it was assumed that the probability distribution $\mu(Z_1Z_2)$ of the Z-coordinates Z_1, Z_2 of the points where the photons scattered could be expressed as a product:

$$\mu(Z_1Z_2) = \mu_1(Z_1)\mu_2(Z_2)$$

Now refer to Figure 6 in which the horizontal dimensions have been expanded by a factor of 20 for clarity. The (Z_1Z_2) distribution of photons which leave the source parallel to AA' can indeed be expressed as a product. The (Z_1Z_2) distribution of photons emitted along BB' can also be expressed as a product. But while the Z_1Z_2 distribution of the AA' photons is non zero for

$$Z_c < Z_1 < Z_a$$

$$Z'_c < Z_2 < Z'_a$$

the distribution of the BB' protons is non zero for

$$Z_c < Z_1 < Z_b$$

$$Z'_c < Z_2 < Z'_b$$

Hence the total Z-distribution, which is the sum of the AA', BB'. . .etc. distributions, is a sum of products and <u>cannot</u> be written as a single product

$$\mu(Z_1Z_2) \neq \mu_1(Z_1)\mu_2(Z_2)$$

In other words, Z_1 and Z_2 are correlated. Since R depends on the correlation between the scattering events, we expect it will be affected.

Now μ can be written as

$$\mu(Z_1Z_2) = (1-\varepsilon_\mu)\ \mu_1(Z_1)\ \mu_2(Z_2) + \varepsilon_\mu\mu'(Z_1Z_2)$$

where ε_μ= the fraction of scattering events of the BB' type. Then it can easily be shown that the expression for R (Equation 7 of this chapter)

$$R = 1 - B\cos 2\phi; \qquad [B = m_1m_2(1-\varepsilon_\phi)]$$

becomes

$$R = (1-B\cos 2\phi)(1+\varepsilon_\mu\xi_{12}) \ .$$

The function ξ_{12}, which depends on e_1, Δe_1, e_2, Δe_2, is difficult to compute, and very sensitive to small misalignments of the scatters. Changing the shape of the scatterers to cylinders would not in itself make $\varepsilon_\mu = 0$. ε_μ could be made zero by making the collimator hole sufficiently small to eliminate BB' type events. (See item 5 of Appendix F.)

Correlations between the X,Y coordinates of the points the two photons scatter will now be considered. From Figure 7 which is drawn out of scale, it is clear that for photons emitted near the center of the source,

$$X_2 \sim -X_1$$

$$Y_2 \sim -Y_1$$

where (X_1Y_1), (X_2Y_2) are the X and Y coordinates of the points where the two photons scatter. That is, (X_1Y_1) and (X_2Y_2) are correlated.

Since R depends on the correlation between top and bottom scattering events, we expect it will be sensitive to these correlations. The solid angles Ω_1, Ω_2 subtended by the detectors D_1 and D_2 at the points P_1 and P_2 depend on X_1 and X_2 respectively (for D_1 and D_2 in the positions shown). Now R depends on these solid angles as follows:

$$R \propto \frac{\langle \Omega_1 \Omega_2 \rangle_{12}}{\langle \Omega_1 \rangle_1 \langle \Omega_2 \rangle_2} = F_\Omega \tag{8}$$

where $\langle . \ . \ . \rangle_{12}$ indicates an average over $(X_1 Y_1 Z_1)$, $(X_2 Y_2 Z_2)$ with $X_2 = -X_1$ and $Y_2 = -Y_1$; $\langle . \ . \ . \rangle_1$ is an average over $(X_1 Y_1 Z_1)$; and $\langle . \ . \ . \rangle_2$ is an average over $(X_2 Y_2 Z_2)$. Assuming

$$\Omega_1 \propto 1/L_1^2, \qquad \Omega_2 \propto 1/L_2^2$$

and performing the average yields:

$$F_\Omega \approx 1-(r/L)^2 \cos \phi \tag{9}$$

where r is the average radius of the photon beam,* L is the distance from the axis to the detector, and ϕ is the relative azimuthal angle of the detectors (in Figure 7, $\phi = 0°$).

The lead slits in front of the detectors (not shown in Figure 7; cf., Figure 1) define azimuthal angles ϕ_1, ϕ_2 with respect to the axis of the collimator. However, the azimuthal angles ϕ_1, ϕ_2 appearing in the theoretical scattering formula are defined with respect to the momenta of the photons. Because the paths of the annihilation photons do not lie always on the axis of the collimator, a definite ϕ_1-ϕ_2 corresponds to a spread of Φ_2-Φ_1 of magnitude $\Delta\Phi$ given by

$$(\Delta\Phi)^2 = \frac{1}{2}\,[1+\cos(\phi_2-\phi_1)]\cdot\frac{r^2}{L^2} \tag{10}$$

This lowers the amplitude of the cos $2(\phi_2-\phi_1)$ term by $2(\Delta\Phi)^2$.

The net effect of Equations (9) and (10) is to change the original form of R, viz.,

$$R = 1 - B \cos 2\phi; \quad \phi \equiv \Phi_2 - \Phi_1; \quad B \equiv m_1 m_2 (1-\varepsilon_\phi)$$

---

*Strictly speaking, r is the root mean square radius of the intersection of the photon beam with the scatterer.

to:

$$R = 1 - B\cos 2\phi + \varepsilon[-\cos\phi + B(1+\cos\phi)\cos 2\phi] \qquad (11a)$$

where

$$\varepsilon \equiv \left(\frac{r}{L}\right)^2 \approx \left(\frac{0.125\ \text{in}}{1.4\ \text{in}}\right)^2 \approx 0.009$$

The steps leading up to this last equation assumed a point source of annihilation photons. But the radius of the source is about half the radius of the photon beam. This weakens the correlation between the scattering points P_1 and P_2 of the two photons. A rough Monte Carlo numerical integration shows that for our geometry, Equation (11a) should be replaced with:

$$R \approx 1 - B(1-0.006)\cos 2\phi - 0.003\cos\phi(1-B\cos 2\phi) \qquad (11b)$$

b. Correction for double scattering in scatterer (ε_m)

Figure 8a shows a false event, in which an annihilation photon scatters twice in the scatterer (at point A and point B). Such events have an angular distribution different from that of the true events, in which the photon scatters only once. However, these false events satisfy all our electronic requirements, in particular the sum-energy requirement.

In order to imitate a true event of given energy E", the scattered photon in the false event must leave the scatterer with energy E" and be directed toward the scatterer. The probability that this will happen is proportional to

$$\int \sigma_a \sigma_b \ell \, dE' + \text{terms of higher order in } \ell$$

where

σ_a = the differential Compton cross section per unit E' for a photon with energy E_o to scatter into an energy E'.

σb = the differential Compton cross section per unit E", for a photon with energy E' to scatter into a photon with energy E".

E_o = the original energy of the photon

ℓ = the length available for the scattering to take place.

δ = a solid angle factor giving the probability that the photon with E" be directed toward the detector.

As Figure 8a shows, the photons with energy E" leave B in a cone (determined by E' and E"). For many directions along the cone, the photons cannot possibly reach the detector, regardless of the azimuthal angle Φ' of the scattering event at A.

The following approximations were made;

1. The scattered photons at A and B were assumed to be distributed uniformly with respect to the scattering angles Φ' and Φ''. This assumption implies that the correlation between the final scattering direction, and the scattering direction of the other photon, was completely destroyed. This is conservative, because in the limit where either the scattering angle Θ' or $\Theta'' \to 0$ this correlation is clearly not affected at all.
2. The Compton cross sections σ_a, σ_b were assumed flat with respect to the energy of the scattered photon. This is already a fairly good approximation, and since we were obtaining an upper limit, the maximum (forward) cross section was used.
3. The scatterer was assumed to be cylindrical in shape with a diameter equal to the average diameter of the real scatterer in the calculation of ℓ; and ℓ was limited to half the length of the scatterer. Then, a rough numerical integration was performed for E" = M/2 (M = electron mass). This energy corresponds to a real event with a scattering angle Θ of 90°.

The result was a 7% contribution of false events with energy M/2. Since these events were assumed to have no directional correlation with the other photon, their effect would be a reduction of the cosine

component of R by 7%. A value of 3.5% ± 3.5% was used in our computations:

$$\cos 2\phi \rightarrow (1 - \varepsilon_m) \cos 2\phi; \qquad \varepsilon_m = 3.5 \pm 3.5\%$$

Also, one expects the spectrum of false events to generally increase at low E'; and one expects peaks near E'' = M/4 and M/2 due to photons which scatter through ~0° or ~180° at A, as shown in (b) and (c) of Figure 8. Further discussion of this point appears in Section IV. A.

c. Correction for finite angular resolution (ε_ϕ)

$G_1^{\Delta\phi}$, the angular part of G_1 (cf., section III. A.) was assumed to be a simple rectangular function

$$G^{\Delta\phi_1}(\Phi_1 - \phi_1) =$$

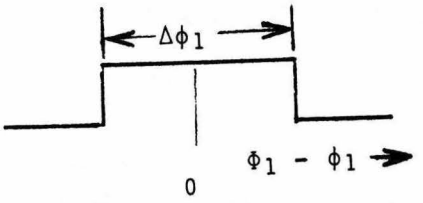

Then, $1 - \varepsilon_\phi(\Delta\phi_1\Delta\phi_2)$ of Equation (7e) of section III. A. becomes

$$1 - \varepsilon_\phi(\Delta\phi_1\Delta\phi_2) = \frac{\sin\Delta\phi_1 \sin\Delta\phi_2}{\Delta\phi_1\Delta\phi_2} \qquad (1)$$

d. Effects of Misalignments.

Misalignment of the collimator hole, scatterers, or the slits defining the azimuthal angles, will generally add cos ϕ and cos 3ϕ term to the cos 2ϕ dependence of R. For example, in Figure 9 the slits have been positioned to determine the angle ϕ around the "aligned" position of the collimator hole, but the hole is actually at the "misaligned" position; the error in the angle is

$$\phi - \phi' \approx \frac{\Delta}{L} \sin\phi \quad (\Delta, L \text{ are defined in the figure}).$$

so the cos 2ϕ dependence changes:

$$1 - B\cos 2\phi \rightarrow 1 - B\cos 2\phi + 2\frac{B\Delta}{L}(\cos\phi - \cos 3\phi) + 0\left(\frac{\Delta}{L}^2\right)$$

Also, when the top collimator hole is misaligned, that portion of the beam emerging from the bottom collimator hole, in coincidence with photons emerging from the top hole, is shifted in the opposite direction.

Similar remarks apply to other types of misalignments. If one of the slits is tilted, the resulting error will depend on the scattering angle Θ of the photon, and hence on the energy of the photon. Similarly, if the scatterer is tilted, the error will depend on the energy of the scattered photon.

Hence we can expect errors in R of order $4B\Delta/L = \delta R$ from misalignments . For our apparatus this is $\frac{\delta R}{\Delta} = \frac{0.03}{mm}$; setting an upper limit of 1 mm misalignment possible misalignment errors of 0.03 in R are obtained.

2. Evaluation of $\bar{m}$ and correction for energy resolution $(\bar{m}_1, \Delta\bar{m}_1)$

To evalaute m in Equation (7) of section III. A., it was necessary to find $G^{e_1\Delta e_1}$ and $G^{e_2\Delta e_2}$. These functions included the effects of the finite energy resolution of the NaI detectors. $\bar{m}_1$ was computed as follows ($\bar{m}_2$ was computed the same way):

Let $h(E_1)$ = the probability, averaged over Z_1, that if the scattered photon has energy E_1, it will enter the NaI detector and contribute to the full energy peak.

It was assumed that the detector had a Guassian response; i.e., that the probability that the pulse from the detector had amplitude e_1 was proportional to $\exp\left[-\left(\frac{e_1 - E_1}{\sigma(E_1)}\right)^2\right]$ where $\sigma(E_1)$ is the standard devia-

tion of the Gaussian. Then the resulting expression for $G^{e_1\Delta e_1}(E_1)$ was

$$G^{e_1\Delta e_1}(E_1) = C \int_{e_1}^{e_1+\Delta e_1} \exp\left[-\left(\frac{e_1'-E_1}{\sigma(E_1)}\right)^2\right] h(E_1)de_1' \qquad (1)$$

where C is some constant. Let

$n_1(e_1) \equiv$ measured spectrum of triple coincidence events $(S_1S_2D_1\Sigma_1)$

$$= n_1\ (e_1\Delta e_1\ \phi\Delta\phi)\Big|_{\Delta e_1 = 1 \text{ channel}}$$

[The experimental values of $n_1(e_1)$ are plotted in Figure 15.] Then $n_1(e_1)$ was written as an integral involving $h(E_1)\cdot f(E_1)$, using Equation (1) above and Equation (4) of Section A. By expanding $h\cdot f$ in a power series, $h\cdot f$ was solved for in terms of $n_1(e_1)$ and the result was substituted in the expression for $\bar{m}_1$ [Equation (7c) of section B] to obtain:

$$\bar{m}_1(e_1\Delta e_1) = \frac{1}{I_n}\left(I_o+I_2\sigma^2+I_4\sigma^4+\ldots\right)$$

where σ = resolution of NaI detector at some convenient energy E_o, and at other energies $\sigma(e) = \sigma e/E_o$,

$$I_n = \int_{e_1}^{e_1+\Delta e_1} n_1(e)de = n_1(e_1\Delta e_1\phi_1\Delta\phi_1) \qquad (5a)$$

$$I_o = \int_{e_1}^{e_1+\Delta e_1} n_1(e)m(e)de \qquad (5b)$$

$$I_2 = \frac{1}{2}\int_{e_1}^{e_1+\Delta e_1} [n_1(e)m''(e)+n_1'(e)m'(e)]\,\frac{e}{E_o}\,de\,. \qquad (5c)$$

The first term, $I_o/I_n \equiv m_1^o$, is the first approximation to m_1. The second term, $(I_2/I_n)\sigma^2 = \Delta m_1$, is the effect of finite detector resolution.

In Equations 5a, b, c the integral signs $\int de$, represent numerical integrations which were performed by summing the integrals channel by channel. The primes (') stand for derivatives which were also evaluated numerically.

C. Construction and Testing of Individual Components

1. Radioactive sources

A 200 μci Na^{22} positron source was used for setup and testing. The main features of the decay scheme, Figure 10 (Le 67) are a 2.6 year half life, a 90% β^+ branching ratio, and a 1.27 MeV gamma accompanying nearly all of the positron emissions. The source was prepared by depositing a water solution of $Na^{22}Cl$ in a depression on a 1 in. diameter 0.2 inches thick lucite disc, evaporating the water, and cementing another lucite disc on top.

Cu^{64} positron sources were used for the data taking runs. Their β^+ activity at the beginning of the runs was ~10 mci. The main features of the Cu^{64} decay scheme, Figure 10 are a 12.8 hour half life, a 19% β^+ branching ratio, and ~1 MeV gamma rays accompanying very few of the positron emissions. The sources were made of 1/8 inch diameter 1/16 inch thick natural copper discs, which were neutron irradiated. Natural copper could be used since it contains 69% Cu^{63}. (The irradiation was performed at the Industrial Reactor Laboratories.)

For energy calibration, we used the 122 keV Co^{57} line and the 511 keV Na^{22} line. Two pairs of sources were made, one for each counter; these pairs were held at standard positions with respect to the counters during calibration runs.

2. Source holder and collimator

a. Design

The source was supported by a brass holder which slid into a rectangular hole in the lead collimator, Figure 2. (This rectangular hole is perpendicular to the plane of the paper.) The positrons were stopped and annihilated in the source and in a thin layer of the surroun-

ding holder material. Holes in the lead of 0.2 inch diameter collimated the annihilation photons; these holes were enlarged to 0.5 inch diameter near the source to avoid the events shown in part b of Figure 2.

b. Testing

If one of the annihilation photons underwent large angle Compton scattering inside the collimator, its momentum would no longer be opposite the other photons' momentum, so both photons could not escape the collimator; hence this event would not be counted, and was of no concern.

A photon could scatter through a small angle in the collimator, emerge, and reach the scatterer. To set a limit on how many did so, we examined the energy spectrum of the emerging photons, using a lithium-drifted germanium detector. We required a coincidence between the Ge detector and a plastic scintillator placed below the collimator as shown in Figure 11. The spectrum was compared to the spectrum taken without the collimator. Most photons which scattered through small enough angles in the collimator to reach the scatterer-position [dashed line in (a)] must have emerged with an energy in the region ΔE shown in part (c) of the Figure. The height Δh of this region was the same for arrangements (a) and (b). Also, the peak width was not noticeably broadened. Therefore, these photons comprised at most a few percent of all those reaching the scatterer position.

Furthermore, photons scattering through such small angles lose only a few per cent of their polarization. Hence, the net effect of small angle Compton scattering in the collimator is only (a few per cent)^2 $\lesssim 10^{-3}$ which is negligible in this experiment.

3. Scatterers

The length of each scatterer was large enough, 1.5", for 33% of the entering photons to Compton scatter; but it was necessary to keep the diameter small to minimize the chance of the photons scattering a second time. (cf. section B. 1. b.).

Our first scatterer, Figure 12b, was 1/4 inch in diameter. It was tested by taking the spectrum of photons which scattered through 90°, leaving 255 keV in the scintillator [see part (c) of the Figure]. A typical spectrum is shown in the same figure.

The low amplitude events were due to photons hitting the phototube. The main peak is broad and asymmetric because light from scattering events near the tip of the scintillator was not collected as efficiently as light from scattered events further up. Therefore this design was rejected.

The next design, Figure 12a, put the light pipe on the side of the scintillator and had the best resolution of all designs tested: 20% full width half maximum (FWHM) for 90° scattered photons (225 keV). However, photons Compton scattering in the light pipe would have introduced serious errors.

We finally settled the design shown in Figure 1d: a conical scatterer surrounded by a slightly larger conical light reflector, coated on the inside with MgO (for efficient, diffuse reflection). Total internal reflection in the scintillator tends to send light toward the light pipe, and the MgO reflects most of the remaining light. The resolution for the 90° scattered photons was 30% FWHM.

4. Azimuthal angle defining slits

Refer to Figure 13. The slits (a) were made of lead and were

0.48 inch thick. The inside edges were "aimed" at the axis of the collimator to minimize the scattering events shown in part (b) of the figure. The top slit and the detector behind it were mounted so they could rotate about the axis of the collimator.

It was necessary to determine the angular widths of the slits in order to compute the correction factor $(1-\varepsilon_\phi)$ discussed in section B.1.c. The widths were measured in two ways:

i. The slit dimensions were measured with a ruler and the following "geometric" widths were obtained:

$$\Delta\phi_1 = 21.8 \pm 1.2^\circ$$

$$\Delta\phi_2 = 19.8 \pm 1.2^\circ$$

ii. The bottom slit was mounted on top of the collimator, with the distance between it and the collimator axis the same as in its original position. [Refer to part (c) of the figure.] A Na^{22} source was mounted on the axis of the collimator, and N_{DD} versus ϕ was measured (where ϕ is the angular position of the top slit and N_{DD} is the rate of detecting annihilation photons in coincidence in the two detectors). [See part (d) of Figure 13.]

The annihilation photons are emitted at 180°, resulting in the N_{DD} dependence shown in (d), and the following "effective widths" were obtained

$$25.90^\circ, \quad 18.50^\circ$$

neglecting the finite size of the source.

As expected these "effective" widths are different from the geometric ones because of finite source diameter ($\sim$ 0.25 inch when the range of the positrons is taken into account), scattering off the sides of the slit, and leakage through the sides of the slit. Substituting

these widths into the expression for ε_ϕ, Equation 1 of section B. 1. c., results in:

$\varepsilon_\phi = 0.050$ (effective slit width at 511 keV with finite source)

$\varepsilon_\phi = 0.060$ (geometric width),

In analyzing our data, the average of these values was used

$\varepsilon_\phi = 0.055 \pm 0.005$.

Hence, $1 - \varepsilon_\phi$ was known to ± 0.5%.

5. Depectors and phototubes

The detectors were 2 inches in diameter by 2 inches long NaI crystals made by Harshaw. The phototubes were Radio Corporation of America (RCA) 8575 bi-alkalai 12 stage phototubes, chosen for their high photoefficiency and fast response.

D. Electronics

1. Description

The function of the electronics was to collect an E_1 spectrum and an E_2 spectrum of the 3-fold coincidence events, an E_1 versus E_2 two-parameter spectrum of the 4-fold coincidence events, and count the total (S_1 S_2) coincidences. The total numbers of 3-fold and 4-fold events were also recorded on scalers.

A simplified block diagram of the electronics is shown as Figure 14. Discriminators connected to the fast outputs of the photomultipliers generated the fast logic pulses S_1, S_2, D_1, D_2. The fast (S_1 S_2) logic pulses were generated by a fast AND (21 nsec resolving time) and counted by a scaler. The fast logic pulses (S_1 S_2 D_1) and (S_1 S_2 D_2) were also generated.

The slow outputs of the photomultipliers were stretched and amplified to form the slow analog pulses s_1,s_2,d_1,d_2. Because of the

high signal rate in the scatterers, the s_1 and s_2 stretchers were gated by the $(S_1\ S_2\ D_1)$ and $(S_1\ S_2\ D_2)$ coincidence pulses respectively. This made it necessary to run the inputs of these two stretchers through delay lines.

The s_1 and d_1 analog pulses were then summed, and the sum was fed to a single channel analyzer (SCA). When the sum pulse was between 0.83 e_m and 1.17 e_m the logic pulse Σ_1 was generated [e_m = 1 electron mass = energy of annihilation photon]. Then the slow logic pulse $(S_1\ S_2\ D_1\ \Sigma_1)$ was generated, and sent to a scaler and the gate of the Y ADC (analog to digital converter) of the MCA (multi-channel analyzer). Similarly, the slow logic pulse $(S_1\ S_2\ D_2\ \Sigma_2)$ was generated and sent to a scaler and the X ADC gate.

The analog pulses d_1 and d_2 were fed to the analog inputs of the Y and X ADC's respectively. The ADC's digitized the signal appearing at their inputs whenever a logic pulse appeared at their respective gates. If one and only one of the ADC gates was opened, the corresponding d_1 or d_2 pulse would be added to the appropriate 1-parameter spectrum. Thus the n_1 and n_2 events (cf. Figure 1) were recorded. If both ADC gates were opened in coincidence (within 1.5 sec), the (d_1, d_2) pulse pair would be added to the 2-parameter spectrum. Thus, the logic requirement on the pulses in the 2-parameter spectrum was $[(S_1\ S_2\ D_1\ \Sigma_1)\cdot(S_1\ S_2\ D_2\ \Sigma_2)$ $= (S_1\ S_2\ D_1\ D_2)\ \Sigma_1\ \Sigma_2$, the desired 4-fold coincidence requirement for the N-events in Figure 1. The 1-parameter spectra did not actually contain all the pulses which satisfied the 3-fold coincidence requirements

---

*s_1, s_2 are the slow outputs of the plastic scatterers; d_1, d_2 are the slow outputs of the NaI detectors.

$[(S_1\ S_2\ D_1\ \Sigma_1),\ (S_1\ S_2\ D_2\ \Sigma_2)]$; the 4-fold coincidence events were missing. The missing events were added later using the computer in the MCA.

The scalers were gated with the "busy" output of the MCA so that they would only count when the MCA was accepting pulses. The multichannel analyzer (model 50/50) was manufactured by Nuclear Data; it contained a Digital Equipment Corp. PDP-8/L computer. The Pegram Nuclear Physics Laboratories electronics staff built the d_1 and d_2 stretchers, SCA's, slow univibrators, slow AND gates, various delay lines, and all the linear amplifiers. The phototube heads were made by the Nevis electronics staff. The fast discriminators, fast AND gates, and the s_1 and s_2 gated stretchers were manufactured by Lecroy.

2. Accidentals, dead time, and pulse pileup corrections.

Accidental coincidences in the various AND gates led to corrections as follows:

Consider R for the total region, i.e., R computed using all valid events regardless of energy. Without corrections for accidentals, R varies as

$$R = 1 + B \cos 2\phi$$

a. Accidentals in the AND gate with inputs S_1, S_2 change B by

$$\frac{\Delta B}{B} \approx \frac{-[S_1]\ [S_2]\ T\ \{S_1,\ S_2\}}{[S_1\ S_2]} = -0.007 \text{ with fresh source}$$

where $[S_1\ S_2] = S_1 \cdot S_2$ coincidence rate

$[S_1]$, $[S_2] = S_1$, S_2 singles rates

$T\ \{S_1,\ S_2\}$ = resolving time of (S_1S_2) AND gate = 21 nsec

b. Accidentals in the AND gate with inputs (S_1S_2), D_1 change B by

$$\frac{\Delta B}{B} = -[S_1]\ T\{(S_1S_2),\ D_1\} = -0.005 \text{ with fresh source}$$

$$T = 95 \text{ nsec}$$

with notation similar to (a). There is a similar correction

$$\frac{\Delta B}{B} = -[S_2]\ T\ \{(S_1S_2)\ D_2\} = 0.005 \text{ with fresh source}$$

$$T = 95 \text{ nsec}$$

c. Accidentals in AND gate with inputs G_1, G_2

Let $G_1 = S_1S_2\ D_1\ \Sigma_1$

$G_2 = S_1S_2\ D_2\ \Sigma_2$

$$\frac{\Delta A}{A} = + \frac{[G_1]\ [G_2]}{[G_1G_2]}\ T\ \{G_1G_2\} = 0.013 \text{ with fresh source}$$

$$T = 2\ \mu\text{sec}.$$

These corrections arose as follows: The accidentals (a) and (b) added events in which the two photons came from different annihilation processes; since the photons were uncorrelated, the effect B was lowered. The type (c) accidentals changed the number of four-fold coincidence events N_{12} without changing N_{SS}, N_1 or N_2 in the expression for R [$= N \cdot N_{SS}/(n_1n_2)$] so they increased A.

Accidentals in the AND gate with inputs $(S_1S_2D_1)$, Σ_1 were negligible because most of the time an $S_1S_2D_1$ pulse is needed to generate the Σ_1 pulse. As shown in Figure 14, it is the S_1S_2D logic pulse that opens the gate, at the input of the stretcher, which generates the s_1 analog pulse, that feeds the Σ amplifier, that feeds the SCA, which generates the Σ_1 logic pulse.

d. Dead-time and pile-up

Dead-time losses and pulse pile-up were calculated to have negligible effect on R.

Chapter IV

Data Reduction and Results

A. Spectrum of the triple coincidence events (n_1 and n_2)

A typical energy spectrum of the triple coincidence events (Fig. 1) is shown in Figure 15 with schematic drawings of events associated with different parts of the spectrum. (The superimposed plot of m(e) will not be used in this discussion.)

True events--in which the photon scatters once in the scatterer and then enters and is fully absorbed in the detector--have energies between e_b and e_d. A typical true event, with a scattering angle θ = 90° has an energy of 0.5 M (electron masses); see (c) in the figure. The scattering angles associated with energies outside the range e_b-e_d are such that the photons cannot possibly hit the detector; cf. (b), (d).

There are two major contributions to the bump at e_a ($e \approx 0.25$ M): [cf. (a)] Events in which the photon which has scattered in the scatterer proceeds to Compton scatter in the detector and escape, thereby leaving only part of its energy in the detector, have a spectrum which would normally extend from 0 to ~0.25 M; except that the lower energy events are vetoed by the sum energy requirement. (A typical sum energy spectrum is shown in Figure 16). In the order of 15% of the events with energy ~0.25 M leak through because of the finite resolution of the detectors. The common event shown, in which a photon scatters through 90° and then backscatters out of the detector, has an energy of exactly 0.25 M.

[cf. (a')] Events in which the photon scatters twice in the scatterer before being totally absorbed by the detector have an energy spectrum which extends from 0.2 to 1.0 M. As pointed out in Chapter III Section

B. 1. b. the spectrum rises at low energies, with peaks expected near 0.25 M and 0.5 M. Thus, these events, especially the event shown as (a') contribute to the 0.25 M bump.

In Chapter III Section B. 1. b. an upper limit of 7% for contribution of false events near 0.5 M was obtained.

B. Comparison of R: Experiment and Theory

1. R for total events (total region)

First R was computed using the total numbers of "N", "n_1", and "n_2" events (defined in Equation 14 of Chapter I and Figure 1). That is, included in N, n_1 and n_2 were all events which satisfied the appropriate time-coincidence and sum energy requirements. The numbers were obtained from the corresponding scalers.

In Chapter III Sections B. 1. a. and D. 2. expressions were derived for corrections to the theoretical R versus ϕ curve, due to finite scatterer diameter and accidentals, respectively. Each experimental value of R was moved by an amount equal in magnitude but opposite in sign to the correction to the corresponding theoretical value of R.* These corrections were small, $\sim$0.01, but comparable to the statistical accuracy. The theory developed in Chapters II and III predicts that after these corrections are made, R exhibits a cos 2ϕ dependence. It was, in fact, found that the experimental values of R could be fit with a curve of the form

$$R = A - B \cos 2\phi \qquad (1)$$

with A = 1.0071 ± 0.0036 (corrected data) and B = 0.3419 ± 0.0051.

---

*The 0.006 B term in Equation 11b of Chapter III section B. 1. a. was omitted from these calculations.

[χ^2/degrees of freedom = 0.84 (10 degrees of freedom: (p = 0.6)]. R versus ϕ is plotted in Figure (4).* Agreement with the expected cosine behavior is excellent, indeed, better than we would have expected, since deviations due to misalignments were estimated to be a few percent. We therefore neglected any error in B due to misalignment.

Next, the predictions of the theory developed in Chapters II and III for A and B was evaluated. The theoretical form of R is

$$R = A - B \cos 2\phi$$

with

$$A = 1 + \Delta A$$

and

$$B = (\bar{m}_1^\circ + \Delta m_1)(\bar{m}_2^\circ + \Delta m_2)(1-\varepsilon_\phi)(1-\varepsilon_m)(1-0.006)$$

where

ΔA = corrections due to Z correlations

$\Delta\bar{m}_1$ $\Delta\bar{m}_2$ = the finite energy resolution corrections

ε_ϕ = the finite angular resolution correction

ε_m = the correction for photons scattering more than once in the scatterer

(1-0.006) results from finite scatterer diameter (See Chapter III section B. 1. a.

m_1, m_2, Δm_1, Δm_2 were found by numerical integrations on the spectra of the triple coincidence events, as per the discussion of Chapter III Section B. 2. The integration used to find these quantities can be viewed as finding the weighted average of m(E) using the n_1 and n_2 spectra as weighting functions.

---

*Data points at the same ϕ have been averaged to facilitate plotting.

Refer again to Figure (15) containing a triple coincidence spectrum and a plot of m(e). The events in and near the bump at e_a, discussed in part A of this chapter, had an unknown angular distribution. Therefore, we used the value of m_1 obtained by integrating from e = 0.33 M to E = M: m = 0.601. Since 0 < m < 0.69 and the events below 0.33 M amounted to 15% of the total counts, the possible error caused by the bump was

$$\begin{cases} + 0.15\ (0.69-0.60) = + 0.0014 \\ - 0.15\ (0.60-0.00) = - 0.09 \end{cases}$$

that is

$$0.51 < m_1 < 0.60$$

or

$$\boxed{m_1 = 0.56 \pm 0.04}$$

similarly,*

$$\boxed{m_2 = 0.58 \pm 0.03}$$

The values of Δm_1 and Δm_2 were found to both be 0.016. The finite angle factor ε_ϕ was already shown in Chapter III, Sections B and C to be

$$\varepsilon_\phi = 4.5 \pm 0.5\%$$

Also, the reduction in the effect due to the annihilation photons scattering more than once in the scatterer was shown in Chapter III Section B. 1. b. to be

$$\varepsilon_m = 3.5 \pm 3.5\%$$

The net result for the theoretical B is

$$B = 0.32 \pm 0.05$$

According to the discussion of Chapter III Section B. 1. a., the Z-correlation would keep B/A constant while introducing uncertainty in A of ~0.05. Thus, the theoretical prediction becomes:

---

*The events below 0.33 M amounted to 8% in the corresponding triple coincidence spectrum.

$$B/A = 0.32 \pm 0.05$$

$$A = 1.00 \pm 0.05$$

There is agreement within the quoted uncertainties between the theoretical and experimental values of A and B/A.

2. R for energy regions

Four energy regions, each representing one possibility of $(e_1\Delta e_1, e_2\Delta e_2)$ [cf. Equation (1a) of Chapter III Section A] are depicted in Figure (3). With the techniques just described R was computed for each region and corrections were applied.

One additional correction was needed. The limits of the energy regions were fixed at certain channels in the MCA, and as the experiment progressed, the actual energies corresponding to these channels drifted by some several percent. To compensate for this, calibration spectra were taken before and after each run; the change in R which was caused by the drift was calculated using the theoretical R versus energy spectrum. The data points were then moved the same amount in the opposite direction. The theoretical and experimental values of the parameters A and B of the fits (Equation 1) are displayed in Table 2. Region 1 was chosen at the maximum of m(E). Since regions 3 and 4 are symmetric when the energies of the two scattered photons are interchanged, the R's of these regions were added.

C. Comparison with the Wu-Shaknov Experiment

In 1950 Wu and Shaknov (Wu 50) measured the Compton scattering of annihilation photons using aluminum scatterers and anthracene detectors. The ratio of two-fold coincidence rates for relative azimuthal detector

angles of 90° and 0° was found to be 2.04 ± 0.12*, as compared with a theoretical value of 2.00 (with no quoted error).

If one assumes a count rate N depending on E_1, E_2, Φ_1, Φ_2, as in Equation (13) of Chapter II Section C:

$$N = f(E_1)\, f(E_2)\, [1-m(E_1)\, m(E_2) \cos 2(\Phi_2-\Phi_1)] \qquad (1)$$

then their results can be interpreted as yielding for B,

$$B \equiv \langle m(E_1)\, m(E_2)\rangle = 0.34 \pm 0.03$$

where the <> indicates an average over the scattering angles of their detectors, compared with a theoretical value of

$$B = 0.33 \text{ (no quoted error)}$$

Wu and Shaknov did not have at their disposal triple coincidence spectra to compute the theoretical B; instead they computed B from their geometry.

Our experiment in addition to measuring B for several energy regions, verified the form of the dependence, Equation 1.

D. Conclusions

Detailed evidence for the theoretical R versus cos 2φ dependence is best provided by the excellent fit to R for the total region (Figure 4), because of its good statistics and freedom from energy versus channel drift uncertainties. Evidence that the magnitude of the cosine dependence is in accordance with the quantum mechanical prediction is provided by the excellent agreement between the theoretical and experimental values of B/A for the energy regions (Table 2). In Figure 5 experimental values of B are graphically compared with the prediction of quantum theory and the upper limits associated with local hidden variable theories and the Bohm-Aharonov hypothesis.

---

*Wu and Shaknov quoted a "mean probable error" of 0.08. We have converted this to standard deviations by dividing by 0.675.

The implications of these results have already been discussed in great detail in the introduction (Chapter I especially Section G).

APPENDIX A

Physical Demonstration that Relative Plane Polarizations of the Annihilation Photons are Parallel or Perpendicular.

The consequence of conservation of parity on a system of two annihilation photons is illustrated in Figure 18. Suppose a linear polarization measurement is made on photon (A) with result $\hat{\varepsilon}$. Then the other photon (B) must have linear polarization $\hat{\varepsilon}'$ either parallel or perpendicular to $\hat{\varepsilon}$. For, if B had a definite direction of circular polarization, (CP) that direction, together with the vector $\vec{r}_{AB}$, could be used to define a right handed screw (See top of the figure). If B has a linear polarization $\hat{\varepsilon}'$, we could define a direction of rotation as that direction needed to rotate $\hat{\varepsilon}'$ so $\hat{\varepsilon}' = \hat{\varepsilon}$, with the restriction that $\hat{\varepsilon}'$ be rotated through the shortest possible angle; this direction and $\vec{r}_{AB}$ define a right-handed screw. This would break down only if $\hat{\varepsilon}'$ is parallel or perpendicular to ε, Q.E.D.

APPENDIX B

Formal Derivation of the Relative Polarizations of Annihilation Photons

It was shown physically in Appendix A that when a positron annihilates with an electron at rest the relative plane polarizations of the two emerging photons must either be parallel or perpendicular. A formal proof that they are perpendicular shall now be offered.

1. Since the positrons annihilate at rest, L = 0 and therefore J = S = 0 or 1 (where L, J, S, = orbital, total spin angular momentum). Consider a final state in which the two photons have equal and opposite momenta along the Z axis. J_Z for each photon can have the value ±1 (units of $\hbar$) corresponding to the two possible helicity states; thus the <u>total</u> J_Z can take on only the values 0, ±2; the values ±1 are excluded because they would require one photon to have $J_Z = 0$. Also, since the maximum S of the electrons was 1, the values ±2 are excluded. Hence, $J_Z = 0$ and the state vector can be written:

$$\Psi = [a^+(k,+1)a^+(-k,+1) + \eta a^+(k,-1)a^+(-k,-1)]|vac> \qquad (B\text{-}1)$$

where $a^+(\vec{k},\pm 1)$ is a creation operator for a photon in a state of ±1 helicity and momentum k; we have used the fact that photons with opposite angular momenta and opposite linear momenta have, of course, the same helicity.

2. It shall now be shown that annihilation from the J = 1, $J_Z = 0$ state is also forbidden. (This step is not essential and the reader may proceed to (3).

Let R_X = a 180° rotation around the X axis. Under R_X the components of a classical electromagnetic field, with right handed circular polarization, given by

$$\vec{A}(\vec{k},+1) = \frac{1}{\sqrt{2}}(\hat{x}+i\hat{y})e^{ikz-i\omega t}$$

transforms to

$$\frac{1}{\sqrt{2}}[(+)\hat{x}+(-)i\hat{y}]e^{i(-k)z-i\omega t} = \vec{A}(-\vec{k}+1)$$

(i.e., $\hat{y}$ and $\hat{z}$ components are reversed). Hence if A is expanded in a Fourier series with coefficients $\alpha_{\vec{k},s}$ (where s = circular polarization)

$$\alpha_{\vec{k},s} \rightarrow \alpha_{-k,s} \quad \text{under } R_X.$$

When the field is quantized, the α's become the operators $a(\vec{k}s)$, so

$$a(\vec{k}s) \rightarrow a(-\vec{k}s)$$

and:*

$$a^+(\vec{k}s) \rightarrow a^+(-\vec{k}s)$$

under R_X.

Hence we see on inspection that the state vector remains unchanged under R_X (using $[a^+(\vec{k}s), a^+(-\vec{k}s)] = 0$ as these are bosons). However, the positron-electron state J = 1, J_Z = 0 transforms under R_X like the spherical harmonic Y_{10}; it changes sign under R_X. Since the Hamiltonian is rotationally invariant (we assume annihilation in free space) this decay of the J = 1, J_Z = 0 state into two photons is forbidden.

Hence, the positrons and electrons at rest annihilate into two photons only from the J = J_Z = 0 state.

3. We now consider the effect of parity transformations on Equation (B-1). Under parity transformations,

---

*Since R_X is a unitary transformation = U,

$$a_{-\vec{k}s} = Ua_{\vec{k}s}U^\dagger \rightarrow a^+_{-\vec{k}s} = Ua^+_{\vec{k}s}U^\dagger$$

upon taking a Hermitian conjugate of each side.

$$x \to -x, \quad y \to -y, \quad z \to -z,$$

$$x + iy \to -x - iy = -(x + iy).$$

The components of a classical field $\vec{A}$ transform like this, so, reasoning as in (B-2) we have:

$a^+(\vec{k},s) \to -a^+(-\vec{k},-s)$ under a parity transformation P

and (B-1) becomes

$$\Psi \to P\Psi = [a^+(-\vec{k}\text{-}1)a^+(+\vec{k}\text{-}1) + \eta a^+(-\vec{k}\text{+}1)a^+(+\vec{k}\text{+}1)]|\text{vac}\rangle \qquad \text{(B-2)}$$

Comparing with Equation (B-1) it is seen that if Ψ is an eigenstate of P with eigenvalue p, then

$$P\Psi = p\Psi \to p = \eta; \quad \eta p = 1$$

so

$$\eta = \pm 1 \text{ for } p = \pm 1 \qquad \text{(B-3)}$$

The creation operators for circular polarization states are related to those for linear polarization states by*

$$a^+(\vec{k}\pm 1) = \frac{1}{\sqrt{2}} [a^+(\vec{k}x) \pm ia^+(\vec{k}y)]$$

$$a^+(-\vec{k}\ 1) = \frac{1}{\sqrt{2}} [a^+(-\vec{k}x) \mp ia^+(-\vec{k}y)]$$

so we have, substituting into (B-2),

$$\begin{aligned} P\Psi = \frac{1}{2} \Big\{ & [a^+(-\vec{k}x) + ia^+(-\vec{k}y)][a^+(kx) - ia^+(ky)] + \\ & + \eta[a^+(-kx) - ia^+(-ky)][a^+(kx) + ia^+(ky)] \Big\} |\text{vac}\rangle \\ = \Big\{ & [a^+(-kx)a^+(kx) + a^+(-\vec{k}y)a^+(ky)][(1+\eta)/2] + \\ & + -i[a^+(-kx)a^+(ky) - a^+(-ky)a^+(kx)][(1-\eta)/2] \Big\} |\text{vac}\rangle \end{aligned} \qquad \text{(B-4)}$$

Hence, if Ψ is an eigenvector of P with eigenvalue p, equations (B-3) and (B-4) yield

$p = -1 \Rightarrow$ ⊥ polarization

$p = +1 \Rightarrow$ || polarization

---

*As before, they are related like the coefficients of the corresponding classical fields.

But it will be shown below that the state of the positron plus an electron at rest has definite, negative parity. Hence, since parity is conserved in the annihilation process, Ψ has negative parity, so the photons emitted in positron annihilation at rest have ~~in~~ polarization.

4. The parity of an electron and positron at rest shall now be derived. The wavefunction of an electron transforms as*

$$\psi(\vec{r},t) \rightarrow \tilde{\beta}\psi(-\vec{r},t)$$

In the representation where the positive energy solution for an electron at rest with spin (up, down) is given by

$$\begin{bmatrix}1\\0\\0\\0\end{bmatrix} e^{imt}, \begin{bmatrix}0\\1\\0\\0\end{bmatrix} e^{imt}$$

and the negative energy solution by

$$\begin{bmatrix}0\\0\\1\\0\end{bmatrix} e^{-imt} \begin{bmatrix}0\\0\\0\\1\end{bmatrix} e^{-imt}$$

(m = the rest energy) the matrix β has the representation:

$$\tilde{\beta} = \begin{bmatrix}1 & & & \\ & 1 & & \\ & & -1 & \\ & & & -1\end{bmatrix}$$

If the wave function of an electron at rest is expanded in terms of these eigenfunctions, the coefficients α,β of the positive and negative energy eigenfunctions transform as follows:

$\alpha_{0\pm1/2} \rightarrow \alpha_{0\pm1/2}$ (coefficient of positive energy solutions)

$\beta_{0\pm1/2} \rightarrow -\beta_{0\pm1/2}$ (coefficient of negative energy solutions**

---

*See any book on relativistic quantum mechanics, eg., J. J. Sakurai, Invariance Principles and Quantum Mechanics, Princeton U. Press, 1964.

**Not to be confused with the β matrix.

where the subscript "0" indicates the electron is at rest, and the ±1/2 refers to the spin. Hence, when these coefficients become operators

$$a(0,\pm 1/2) \rightarrow a(0,\pm 1/2)$$

$$b^{+}(0,\pm 1/2) \rightarrow -b^{+}(0,\pm 1/2)$$

Hence, the initial electron state, constructed to have J = 0

$$(a^{+}(0+1/2)b^{+}(0-1/2) - a^{+}(0,-1/2)b^{+}(0,+1/2)] \,|\text{vac}\rangle$$

has negative parity.

APPENDIX C

Bell's Counter-example Showing that this Experiment Cannot Rule Out Local Hidden Variable Theories.

Let the first photon scatter with probability

$$d\Omega_1[F(\Theta_1) - \sqrt{2}\, G(\Theta_1) \cos 2(\Phi_1 - \lambda)] \qquad \text{(C-1)}$$

and the second with probability

$$d\Omega_2[F(\Theta_2) + \sqrt{2}\, G(\Theta_2) \cos 2(\Phi_2 - \lambda)] \qquad \text{(C-2)}$$

where λ is a hidden variable uniformly distributed between 0 and 2π; and Θ, Φ, Ω are the usual polar, azimuthal, and solid scattering angles. If further

$$F(\Theta) = [(1 - \cos \Theta)^3 + 2]/(2 - \cos \Theta)^3$$

$$G(\Theta) = \sin^2 \Theta/(2 - \cos \Theta)^2$$

and the joint distribution is obtained by multiplying expression C-1 by C-2 and averaging over λ, the quantum distribution [see e.g., Pryce and Ward (Pr 47)] is obtained.

This model is acceptable because it happens that the expressions C-1 and C-2 are always positive, as probabilities must be. For photons of somewhat lower energy the required expressions are not always positive and this type of model fails. (The other counter-example in I. E. is not subject to this restriction.)

APPENDIX D

P(ab) Evaluated According to the Bohm Aharonov Hypothesis; and the Relation* of the Hypothesis to Local Hidden Variable Theories.

Suppose a linear polarization analyzer gives the responses +1 and -1 for photons linearly polarized parallel and perpendicular to its axis. The average response of the analyzer to an elliptically polarized photon represented by the vector $e|x'> + if|y'>$, with e and f real, is given by

$$\zeta(a,\beta) = (e^2-f^2)\ [\cos^2(a-\beta) - \sin^2(a-\beta)] \qquad \text{(D-1)}$$

where a is the direction of the analyzer axis and β the direction of the $\hat{x}'$ axis; and the normalization $e^2 + f^2 = 1$ has been used.

Consider the following mixture of 2-photon states. Photon 1 is characterized by e, f, β, and photon 2 by e', f', β'; β is uniformly distributed between 0 and 2π, and $\beta' = \beta$. For this mixture, P(ab) is given by

$$\begin{aligned} P(ab) &= \int_0^{2\pi} d\beta \frac{1}{2\pi}\ \zeta(a\beta)\ \zeta(b\beta') \\ &= (e^2-f^2)(e'^2-f'^2)\ \frac{1}{2}\cos 2(a-b) \end{aligned} \qquad \text{(D-2)}$$

Evidently, all ensembles possessing the rotational and reflective symmetry hypothesized by Bohm and Aharonov must be sums of such mixtures.** Also, $|e^2 - f^2| \leq 1$. It follows that for any BA mixture

$$P(ab) = C \cos 2(a-b) \qquad \text{(D-3)}$$

with $$|C| \leq \frac{1}{2}$$

Furthermore, comparing equation D-2 with equation 5 of Chapter I shows that the expression for the results of measurements on the BA

---

*We thank R. Friedberg for pointing out the relation.

**BA assumed $\beta=\beta'$. If $\beta'=\beta+\theta$ in (D-2), reflective symmetry requires adding adding a mixture with $\beta'=\beta-\theta$, and (D-3) still holds.

mixture considered has been put in the same mathematical form as a local hidden variable theory. Clearly, the general mixture can also be written in such a form.

APPENDIX E

Experimental Evidence for the Validity of the Quantum Relations Between Compton and Ideal Polarization Analysis

It has been assumed that the quantum prediction for the function relating Compton and ideal polarization measurements is correct. This assumption is supported by measurements of:

A. The angular distribution of Compton scattered polarized photons.

B. Atomic energy level spacing and g factors of the electron and muon.

C. High energy electromagnetic scattering cross sections and angular distributions.

These will now be considered in turn.

A. Angular distribution of Compton scattered polarized photons.

The methods available for producing beams of polarized photons include Compton scattering of unpolarized photons and bombarding a polarized laser beam with a high energy electron beam. Experiments in which such beams of polarized photons were Compton scattered shall now be described.

1. Suppose a beam of unpolarized photons is Compton scattered twice, as shown.

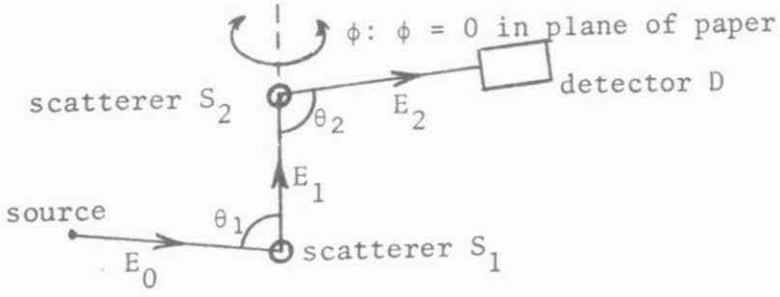

The successive scattering on scatterers S1 and S2 reduces the original beam energy E_o to E_1 and then to E_2 as shown. The first Compton scattering gives the beam a partial linear polarization (Ev 58). The beam is

scattered again, and the dependence of the intensity as a function of ϕ is compared with the quantum prediction. It is easily seen that the intensity is proportional to $1 + \rho m(E_2) \cos 2\phi$ where ρ is a measure of the polarization produced by the first scattering and m is a quantity defined in Chapter 1.*

Hoover et al. (Ho 52) measured the S_2D coincidence rate normalized to the $\phi = 0$ value. (They used $\theta_1 = 50$ and $83°$, $\theta_2 = 90°$, and $\phi = 30, 50, 70$, and $90°$. The source was Co^{60}, giving a mixture of 1.17 MeV and 1.33 MeV gamma rays.) Discrepancies of as much as 3.6 (statistical) standard deviations between theory and experiment were found. This would correspond to as much as a 25% discrepancy in m if m were assumed to be solely responsible. However, the authors believed the discrepancy was probably due to instability of the electronics.

Singh et al. (Se 65) improved on the experiment several ways. They used a thin copper scatterer for S_1 to minimize multiple scattering in S_1. A plastic scintillator was used for S_2 and NaI was used for D; and single channel analyzers checked if the appropriate energies were deposited in S_2 and D. Rates were normalized to the $\phi = 0$ rate. Measurements were made at $\theta_1 = 64, 90, 120°$; $\theta_2 = 90°$; $\phi = 0, 30, 50, 70, 90°$; and $E_o = 280$, 662, and 1250 keV.

Scatterers of two different thicknesses were used and gave results that agreed within statistics, so any effect of multiple scattering of gamma rays in the scatterer was small. The spread $\Delta\theta_1$ and $\Delta\phi_1$ in θ_1 and ϕ_1 were small enough to have a negligible effect.

---

*See Equation (8). m also depends on E_1, of course. See Si65 (for example) for the dependence on the angle θ_1.

The spreads $\Delta\theta_2$ and $\Delta\phi_2$ in θ_2 and ϕ_2 were larger, (35-55°) and there were ±5° uncertainties in these spreads. It can be shown that these ± 5° uncertainties cause less than a 5% uncertainty of the average (over θ_2 and ϕ_2) of the theoretical value of m. Also, the 36 values of counting rates (normalized to ϕ = 0) agreed with theory within statistical uncertainties of 1-3%.

The implications of these results depend on how hypothesized variations of m from theory are parameterized. Suppose m is changed to $(1 + \delta)m$ (δ = a constant), for example. Then the statistical uncertainties alone would imply $\delta \lesssim 2\%$; while uncertainties in $\Delta\theta_2$ and $\Delta\phi_2$ (noted above) would, alone, imply $\delta < 5\%$; therefore $\delta \lesssim 7\%$. Furthermore, the agreement between theory and experiment, with respect to the detailed E_o, θ_1, ϕ_2 dependence, provides confidence that the theory is accurate to better than this 7% figure.

The experiment was also repeated by Raju et al. (Ra 68). Like Singh et al. they looked at the energy deposited in S_2 and D. In contrast to Singh et al., they used two D's simultaneously, one at ϕ = 0° and the other at ϕ = 30, 60, or 90°; and tabulated the ratio r of rates in the two D's. Also, they used NaI for S_2 and 1/2" x 1/2" Al for S_1. (Their single channel analyzers looked at the sum of energies deposited in S_2 and D, and the energy deposited in D. They used θ_1 = 45, 60, 75, 90°; θ_2 = 90°; and E_o = 662 keV.)

The experimental value of r (defined in the above paragraph) agreed with theory to within 10% at all values of θ_1 and ϕ. The authors claimed this was consistent with 5% statistical and 5% experimental uncertainties in r.

They failed to note, however, that the experimental r is systematically smaller by ~10% in every one of the 12 conditions. It is easy to see from the above that the average discrepancy in r is about 10%, with a systematic uncertainty of ~5% and a statistical uncertainty of 5/ $\sqrt{12}$%. Such a discrepancy is <u>not</u> consistent with zero; a systematic discrepancy of (10-5) ± 5/ $\sqrt{12}$% = 5 ± 1.4% is not accounted for. This would correspond to about a 16 ± 4.5% discrepancy in $m(E_2)$, assuming the polarization due to the first scattering is correctly given by theory.

The reason for this discrepancy is probably multiple scattering in S, which Raju et al. claimed was not excessive. According to a rough estimate, (along the lines of the calculation in Chapter III section B.1.6.), such multiple scattering produces an effect with the same sign and the same order of magnitude as the discrepancy.

2. Suppose a high energy electron beam interacts with a polarized laser beam of optical photons. In the rest frame of the electrons, this is equivalent to a polarized X-ray beam Compton scattering on the electrons. The laser beam polarization may be measured with optical analyzers, which are nearly ideal. Hence a comparison of ideal and Compton scattering measurements on single photons could be made.

Facilities for electron-laser beam bombardment have been constructed at SLAC (Si 69) CEA (Sa 69) and in Russia (Ku 67). Unfortunatately, the angular distribution of the scattered electrons or (equivalently) the scattered photons, has not been measured.

B. Atomic energy level spacing and g factors of the muon and electron.

Compton scattering is computed, of course, using quantum electrodynamic theory (QED). Evidence for the validity of QED has been reviewed

by Brodsky and Drell (Br 70). The g factors of the electron and muon have been computed using the value of the fine structure constant obtained from the A. C. Josephson effect. The theoretical values of g-2 agree with experiment within the theoretical and experimental uncertainty, totaling about 30 parts per million (ppm). The agreement between theoretical and experimental values of g-2 for the muon is about 300 ppm. Also, the agreement for the Lamb shift is in the order of 100 ppm.

Although the agreement between theory and experiment is impressive, these experiments should be supplemented by experiments which are more closely related to Compton scattering and which involve energies equal to or greater than those of annihilation photons. Suitable experiments shall now be discussed.

C. High energy electromagnetic scattering processes.

The process

$$e^+e^- \rightarrow 2\,\gamma$$

has been studied at high energies using colliding beams of electrons and positrons. This process has the Feynman diagram of Compton scattering, "turned on its side":

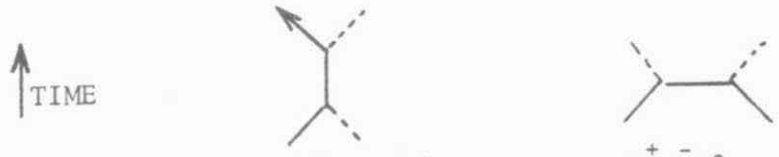

Compton Scattering $\qquad$ $e^+e^- \rightarrow 2\gamma$

Bacci et al. (Ba 71) have measured the cross section for values of θ near 33° ("small") and 90° ("large")

and single beam energies of 0.7 to 1.2 keV. The ratio of large angle to small angle cross sections agreed with theory to within the experimental and theoretical uncertainties (of about 20% each) for 4 values of beam energy. The ratio of the total cross section to small angle e^+e^- scattering agreed with theory within 20% experimental uncertainties. Balakin et al. (Bal 71) measured the (2γ annihilation/elastic scattering) ratio at ~90°, and single beam energies of 500 MeV and 510 MeV. The experimental and theoretical values of the ratio agreed to within the corresponding experimental uncertainties (of 13% and 9% respectively).

Other high energy scattering experiments are reviewed in Brodsky and Drell (Br 70). In particular, the total Bethe-Heitler cross section for pion production and bremstrahllung have been found to agree with theory to within 1% at energies up to 3.6 GeV. These processes also have Feynman diagrams similar to that of Compton scattering:

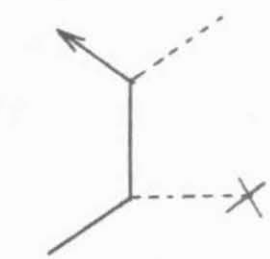

Bremstrahlung

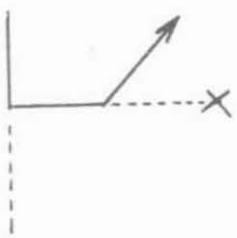

pair production

Conclusion

These experiments provide supporting evidence that the relation between Compton and ideal polarization measurements is correctly given by Quantum mechanics. The double Compton scattering experiment of Singh et al. provides evidence that theory correctly predicts m at least better than 7%; the agreement between theory and experiment for the detailed dependence on energy and angle provides confidence that the theory is even more accurate than that.

The experiments on high energy experiments and the precision atomic experiments are much more precise, although they are less directly related. The most direct test--using scattering of high energy electrons on a laser beam--has not yet been performed.

It should be mentioned that the relation between Compton and ideal measurements on polarization correlations between two photons might not be correct even if experiments--such as the above--verified the relation for measurement on single photons. This is because of the possibility of "hidden variables", associated with the two photons, which are correlated in such a way that they affect polarization correlations but not measurements on single photons.

Nevertheless, these experiments taken together provide strong evidence that quantum theory is an accurate description of the Compton scattering process.

APPENDIX F

Possibility of Improved Accuracy

If a more accurate and complete measurement of the Compton scattering of annihilation radiation is necessary, the following steps can be taken:

1. Using Na^{22} for the source would permit long runs at a stable counting rate; all other factors remaining constant, a 1 month run using a 10 mci Na^{22} source would provide ~15 times the number of counts we obtained with our two runs, each of which nearly exhausted a 10 mci Cu^{64} source. (The half-life of Cu^{64} is 12.8 hours).
2. Reducing the source diameter from its present value of 0.125 in to 0.06 in would increase the counting rate by a factor of ~3, because the solid angle available for both annihilation photons to leave the collimator decreases with the distance r' from the point the photons leave the source to the collimator axis.
3. A detailed calculation of the effect on R, of photons which scatter more than once in the scatterer would eliminate an uncertainty of $\sim\pm 1\%$ in R. The size of this correction could be made smaller by reducing the radius (r) of the scatterer, but this would reduce the counting rate (which is proportional to r^2).
4. A collimator hole in the shape of a cone, Figure 17a, (cf. with Figure 6) combined with the smaller diameter source (item 2 above) would result in a better defined beam.
5. Choosing the minimum diameter of the scatterer larger than the beam

diameter* would eliminate the z-correlation effect described in Chapter III section B.1.a. Also, alignment of the scatterer would no longer be as critical: As long as the beam remains sufficiently inside the scatterer, any misalignment only affects the correction factor involving photons which scatter more than once inside the scatterer. (cf., Item 3 above.)

6. Using 2 in diameter x 5 in long NaI crystals for detectors, positioned as in Figure 17b, would greatly increase the range of scattering angles Θ, and hence the range of energies, of the scattered photons that were accepted.

7. A calculation of the polarization dependence of the detectors would eliminate another source of uncertainty. The polarization dependence arises from the fact that there is a comtribution to the full energy peak from photons which enter the detector and Compton scatter. Near a surface of the detector, the chance that the scattered photon is absorbed depends on its direction. The direction is related to the initial polarization; hence the detector is sensitive to the polarization. This is an $\sim$10% effect for 255 keV photons moving parallel to and within $\sim$1 cm of a detector surface. Proper geometry could minimize this effect.

---

*The scatterer diameter would have to be larger than the beam diameter by an amount at least equal to the range of the recoil Compton electrons, because the energy of these electrons must be fully absorbed by the scatterer for the sum energy requirement to be satisfied. In Figure 6 the horizontal (X) distance between the dashed lines and the outside of the scintillator $\approx$ this range.

If steps 1-7 were carried out, a 1 month run with a 10 mci Na^{22} source would produce $\sim$ 0.001 statistical accuracy in R for each point in the total region, and $\sim$0.003 statistical accuracy in each of the 9 energy regions. Systematic uncertainties in R would be $\leq$ 0.003 everywhere assuming a calculation of the multiple scattering in the scatterer and the polarization sensitivity of the detector could be computed to $\sim$5% and the apparatus were built to 0.1 mm. This would be an improvement of a factor of $\sim$10 over the present experiment.

Of course, only certain of steps 1-7 need be applied if a special feature of the scattering is to be tested.

$\cos 2\phi$	Run No.	R, Uncorrected	ΔR, Finite Diameter	ΔR, Accidentals ΔA	ΔR, Accidentals $\Delta B \cos 2\phi$	R, Corrected
-1	13	1.344 ± .018	0.000	-.002	.002	1.344
	3	1.355 .013		-.007	.007	1.355
-0.5	11	1.189 .014	.002	-.006	.003	1.188
	12	1.177 .015		-.004	.002	1.177
	5	1.159 .019		-.002	.000	1.159
0	14	0.982 .017	.002	-.002	.000	0.982
	2	1.004 .011		-.010	.000	0.996
	10	1.029 .009		-.009	.000	1.022
0.5	15	0.823 .019	.002	-.001	.000	0.824
	4	0.836 .012		-.003	-.001	0.834
1	1	0.694 .001	.002	-.013	-.012	0.671
	6	0.665 .014		-.002	.000	0.665
	9	0.685 .010		-.012	-.012	0.663

Table 1. R for total events, and corrections, ΔR.
Cf. section IV B.1.

Region	Theory A	Theory B/A	Experiment A	Experiment B/A	χ^2/n'
1	1.00 ±.05	0.415 ±.015	1.021 ±.010	0.409 ±.018	1.1
2	1.00 .05	0.372 .010	0.984 .019	0.392 .030	.7
3+4	1.00 .05	0.395 .015	1.020 .010	0.390 .017	1.5

(n'=degrees of freedom=2)

Table 2. Comparison of experimental A and B/A with theory.
See section IV B.2.

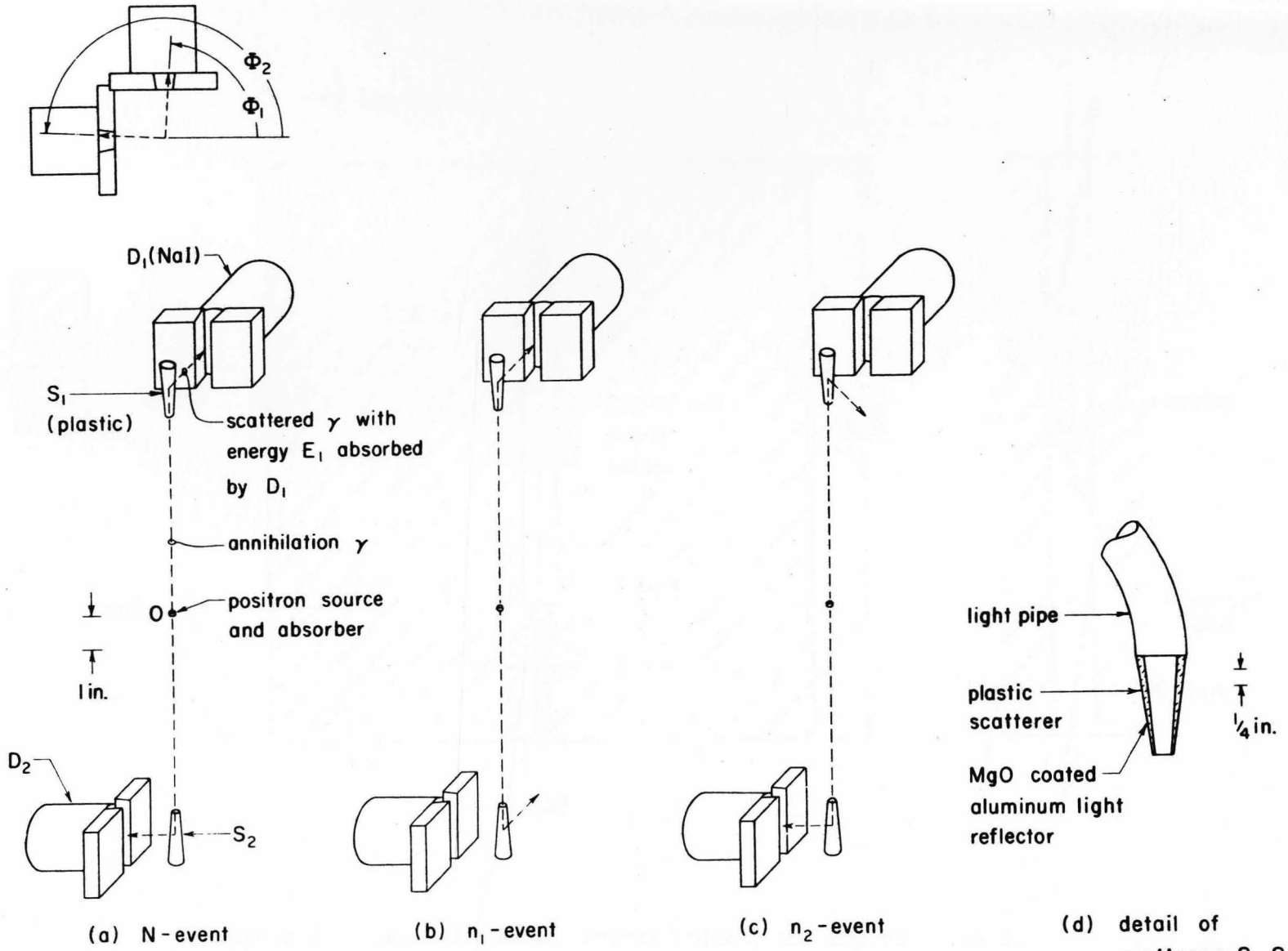

Figure 1. Schematic view, to scale, of the experimental arrangement. The lead collimator is omitted. (a) four fold coincidence event; (b), (c) three fold coincidence events; (d) detail of scatterers.

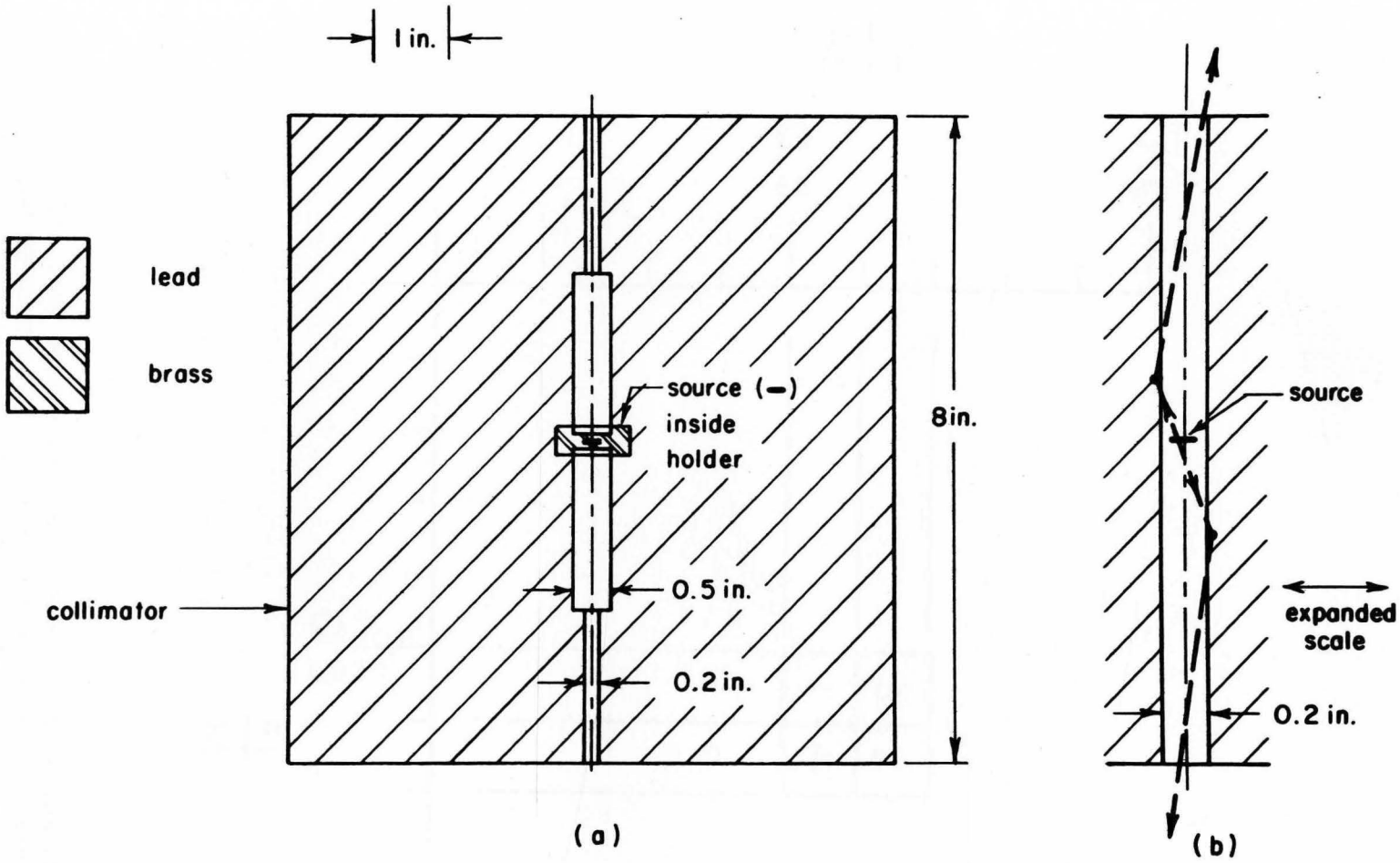

Figure 2. (a) Collimator, source holder, and source. The 0.5 in diameter cavity prevents events of the type shown in (b). Note the expanded horizontal scale in (b).

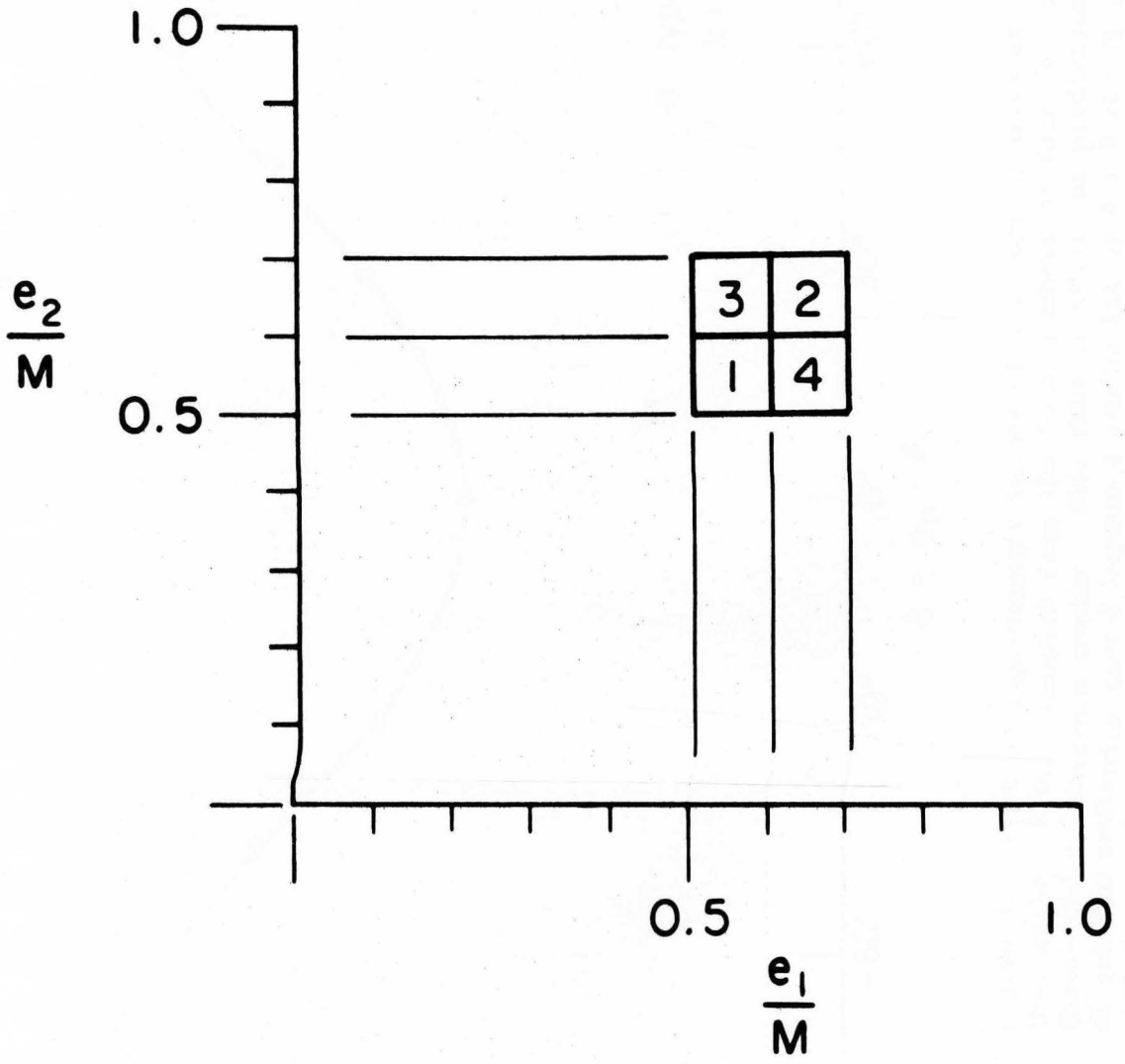

Figure 3. The four energy regions chosen to study the amplitude of the cosine dependence of R. The quantities e_1, e_2 are the energies of the scattered photons; M = 1 electron mass.

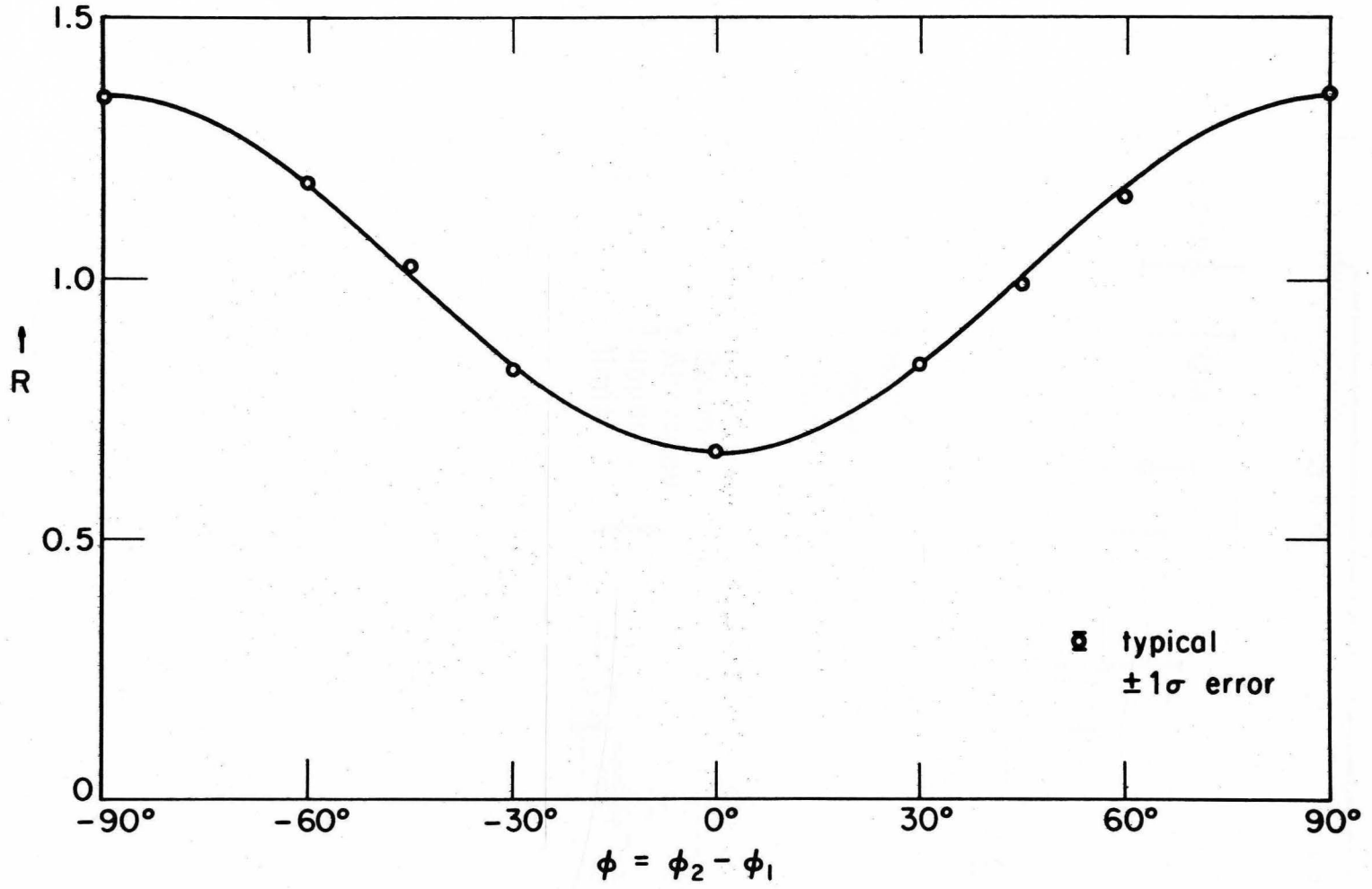

Figure 4. Plot of experimental values of R versus relative azimuthal angle. R was computed from the total numbers of four-fold and three-fold coincidence events. This data verifies the prediction of quantum mechanics that R versus ϕ can be fit by $A + B \cos 2\phi$, with A, B, adjustable. The best fit is shown as solid line (X^2/ degrees of freedom = 0.84).

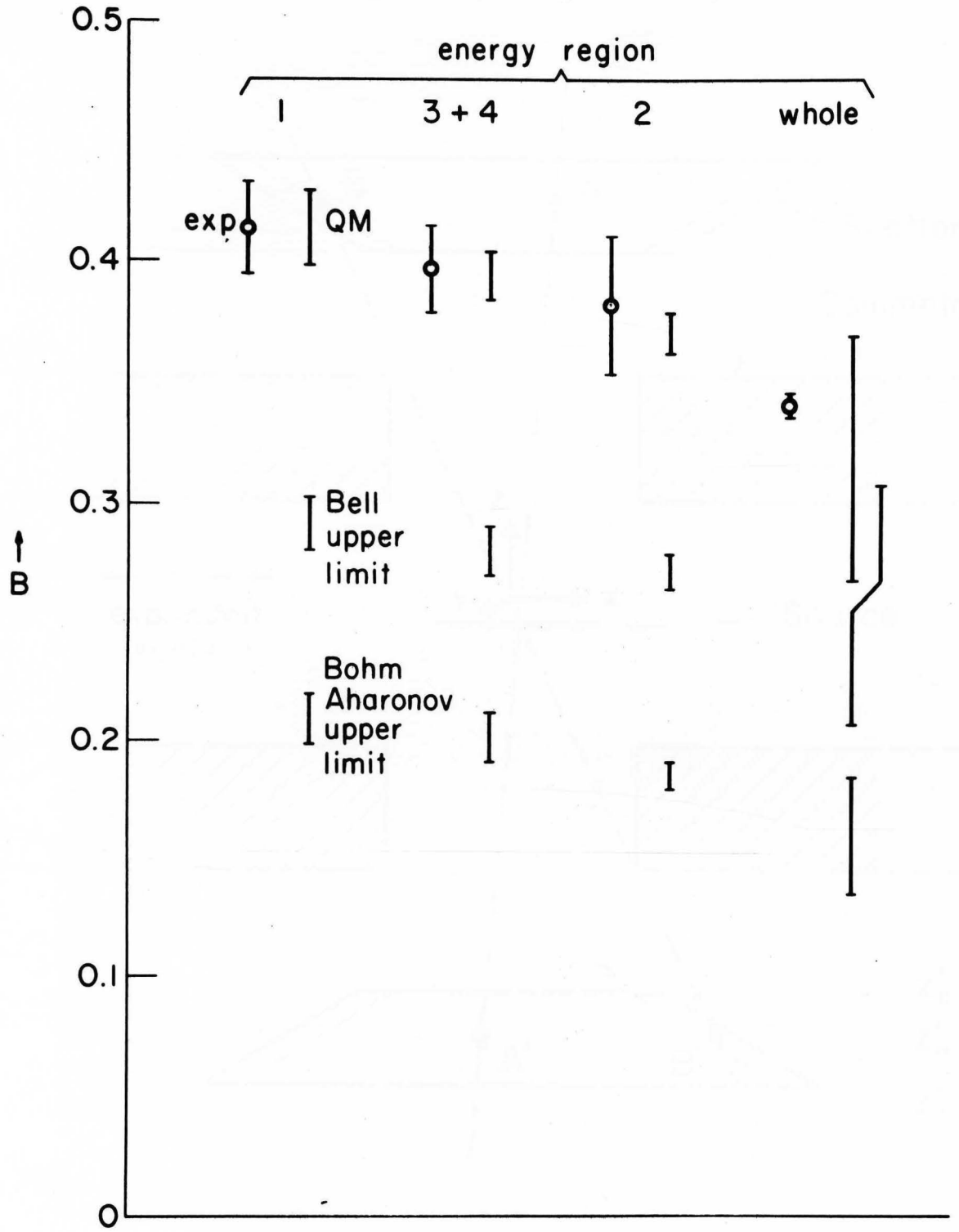

Figure 5. Comparison between experimental (exp) results and quantum (QM) predictions for B, and the upper limits on B derived from Bell's inequality and the Bohm Aharonov hypothesis. The error bars on the experimental points indicate uncertainties in instrumental corrections of the various theoretical predictions.

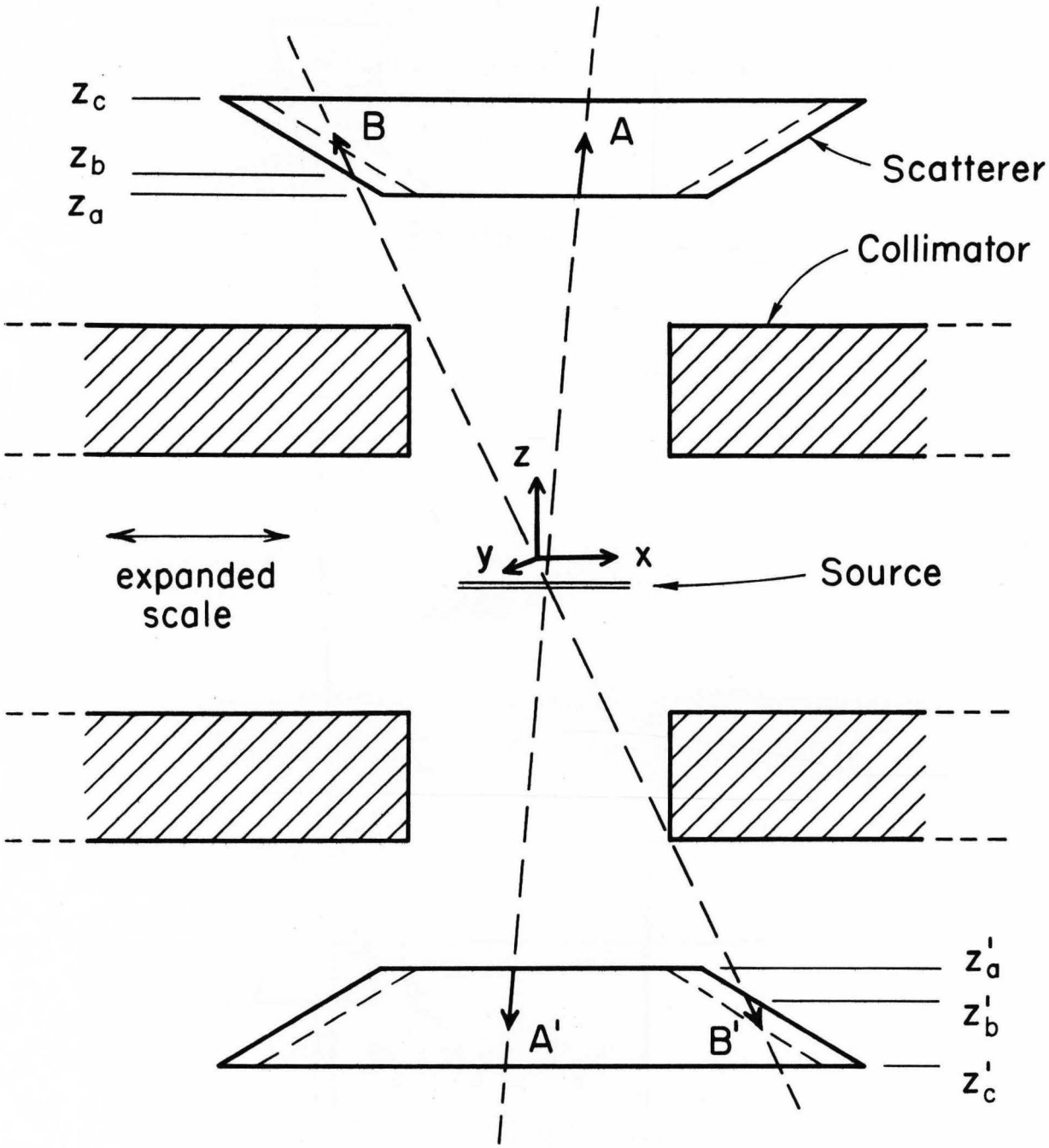

Figure 6. Source, collimator, and scatterer drawn with horizontal scale expanded 20x. This figure illustrates the correlation between the Z coordinates of the points where the two photons scatter.

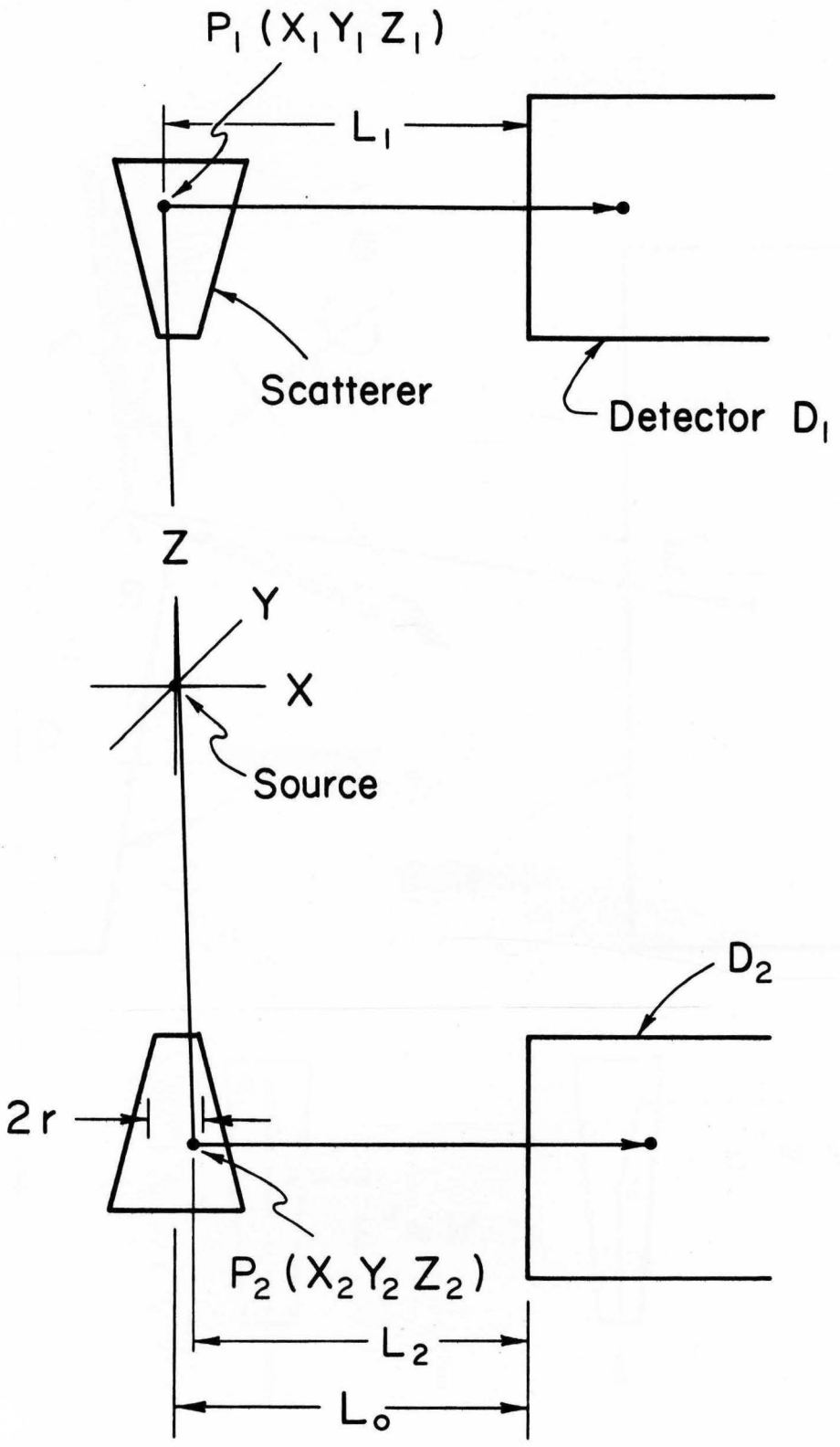

Figure 7. The X and Y coordinates of the points P_1 P_2, where the two photons scatter, are correlated.

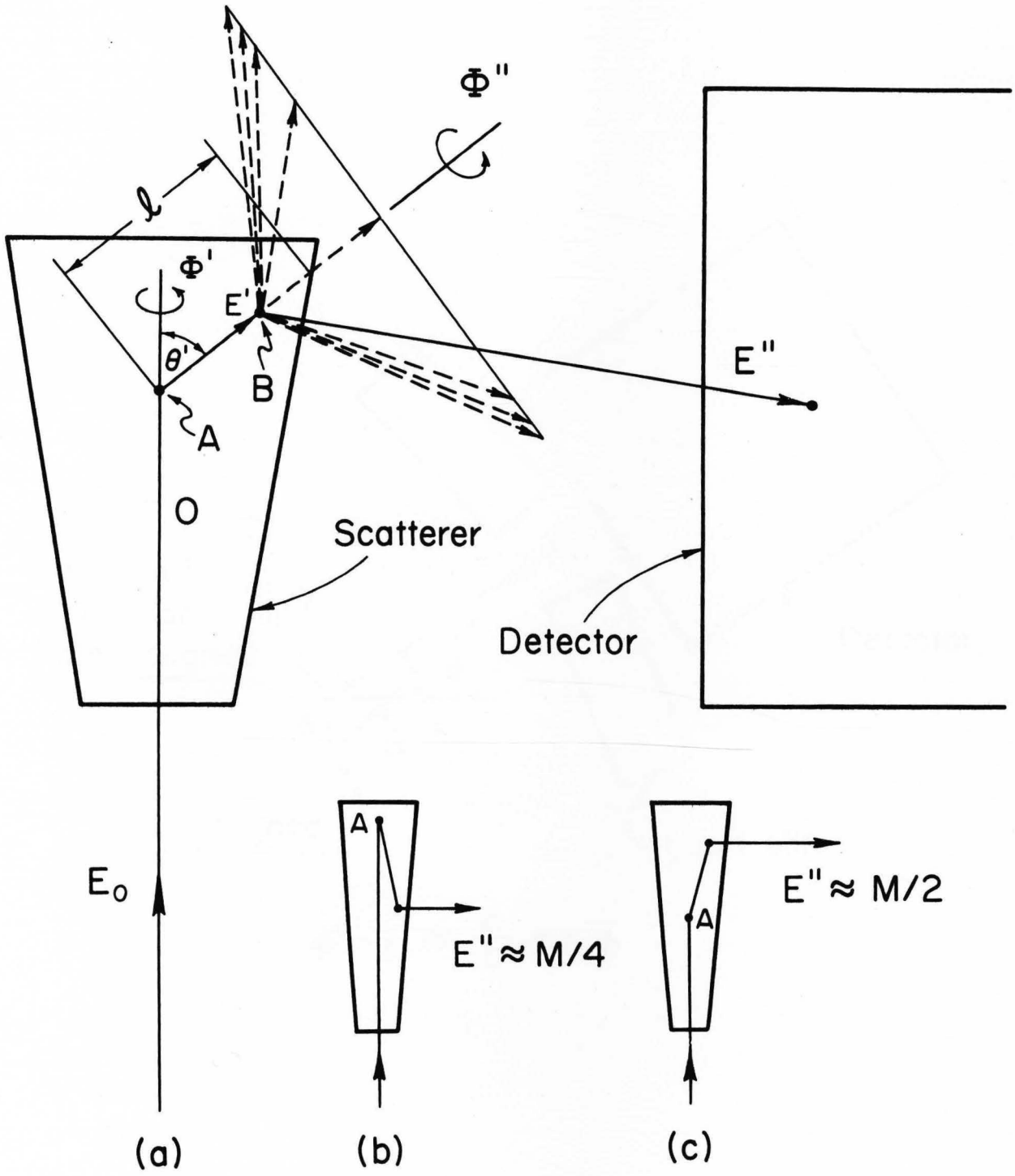

Figure 8. Photons which scatter twice in the scatterer, having energy E' between scatterings, and emerging with E''.

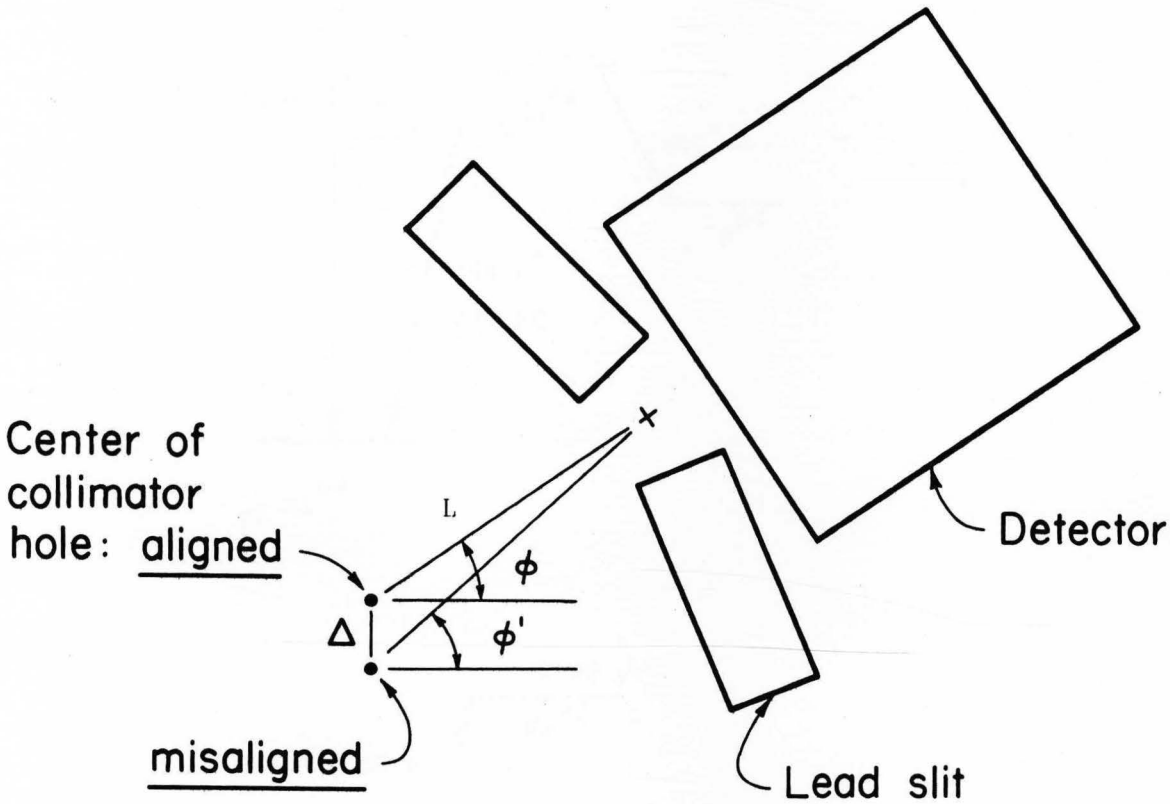

$$\phi' - \phi \approx \frac{\Delta}{L} \sin \phi$$

Figure 9. Effect of collimator hole misalignment.

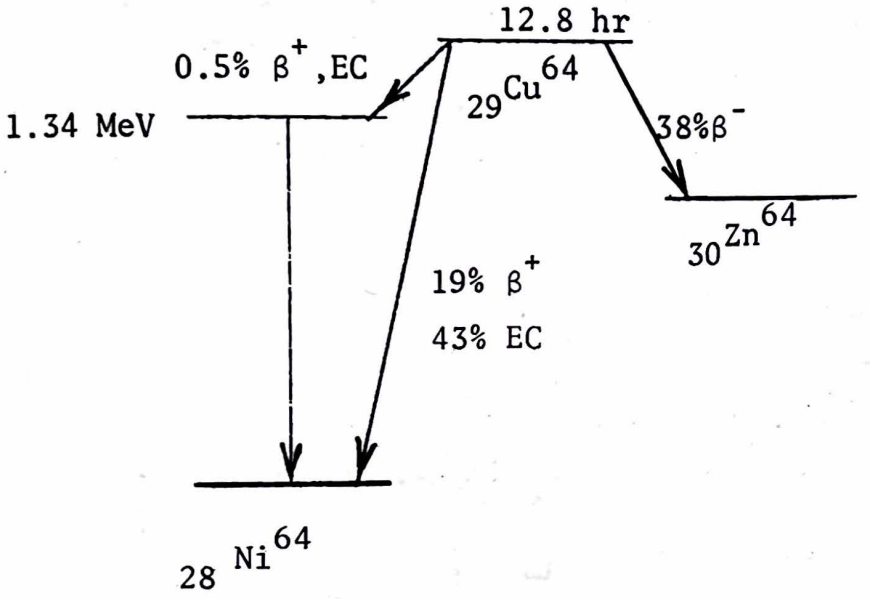

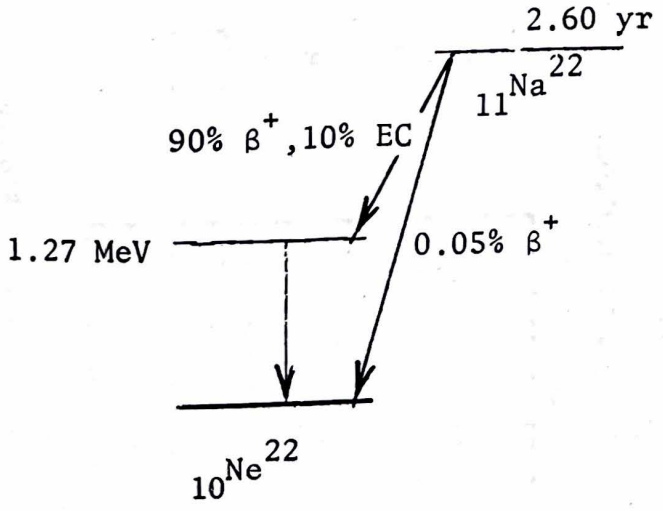

Figure 10. Decay schemes of Cu^{64} and Na^{22}.

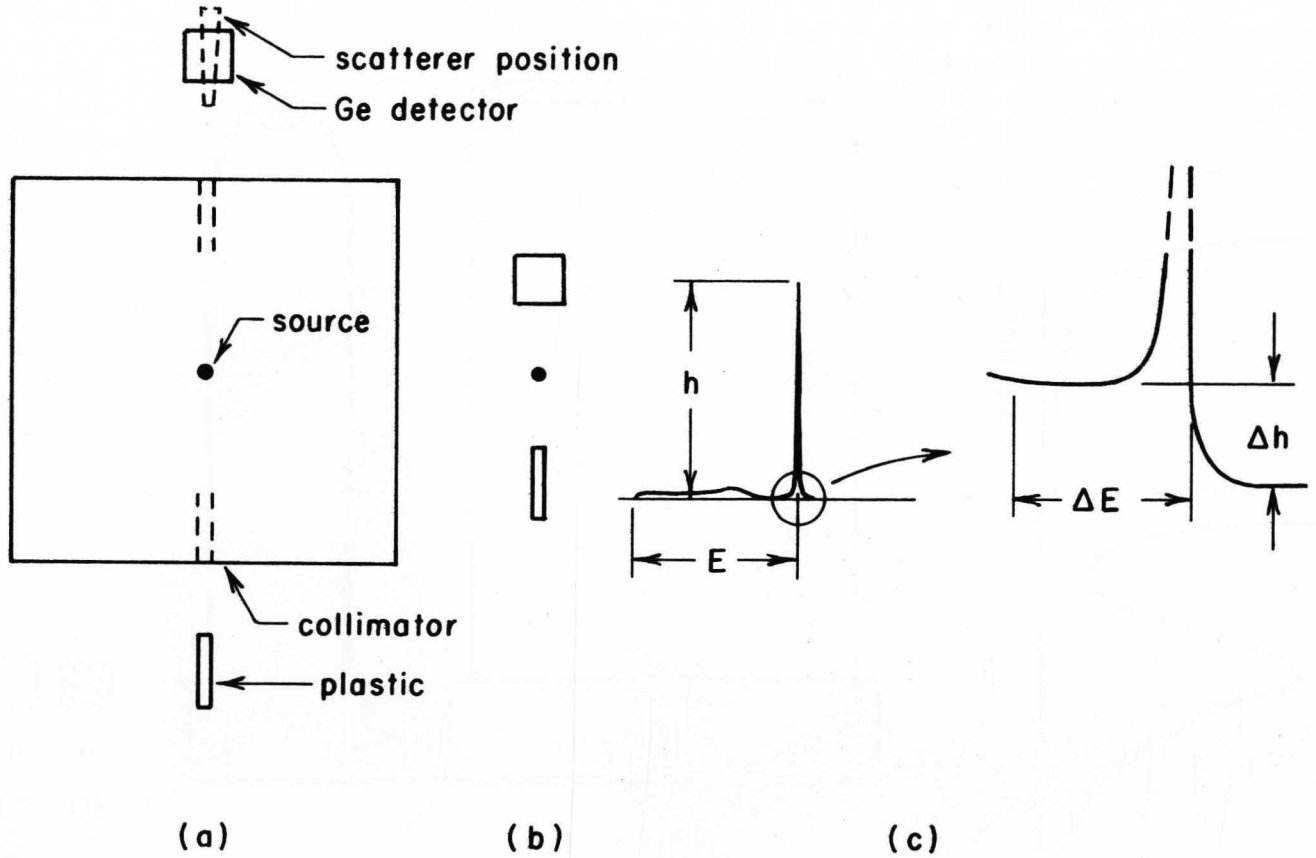

Figure 11. Testing for small angle Compton scattering in the collimator. The spectrum in the Ge detector, gated by the plastic scintillator, is taken with the source inside the collimator, (a) and without the collimator, (b); the spectrum, (c), is compared for the two cases. The results shown that small angle scattering affected R by less than 10^{-3}.

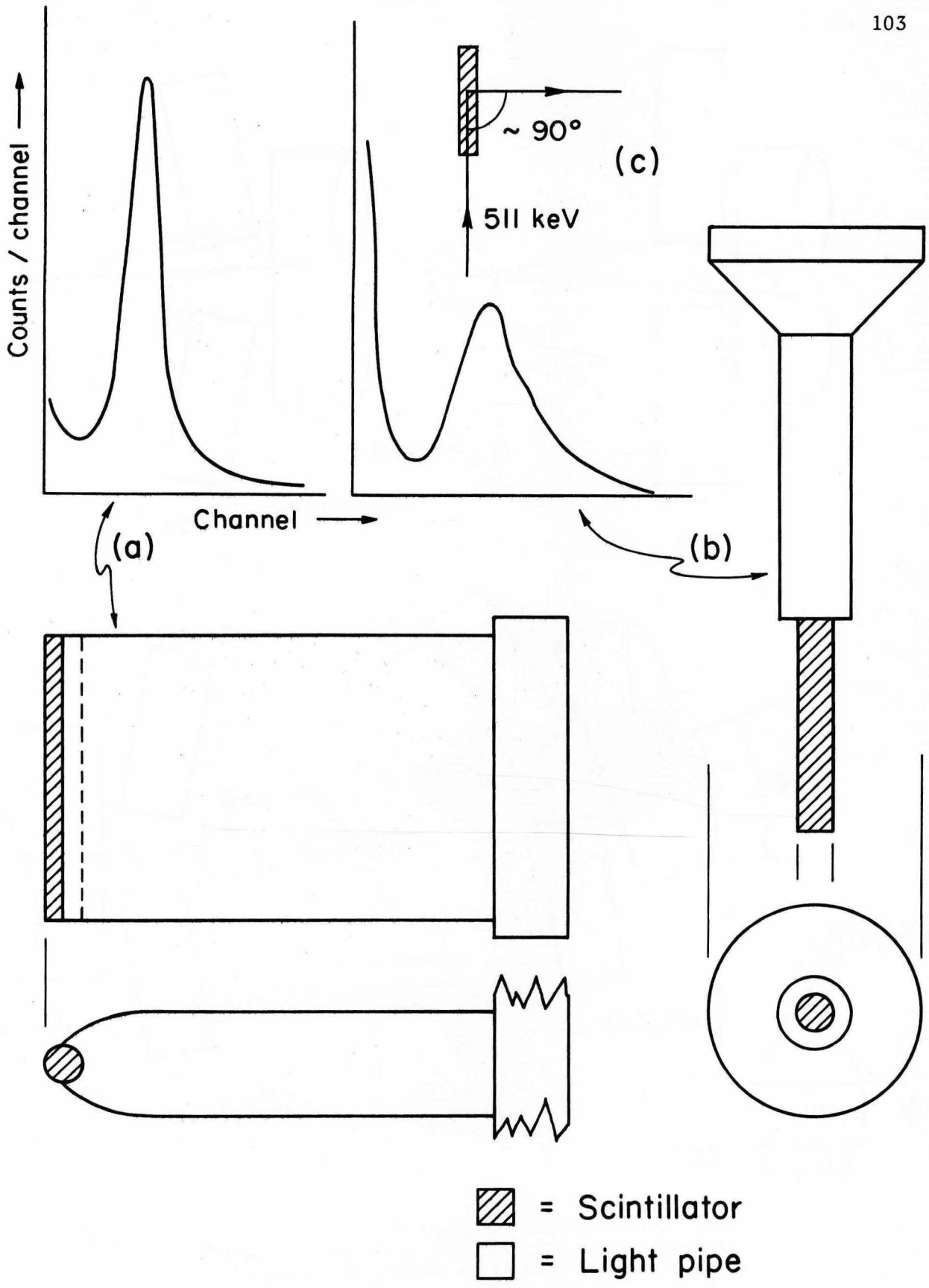

Figure 12. (a), (b); Two preliminary designs for the scatterers, shown with spectra of 90° scattered 511 keV photons (c). Final design is shown in Figure 2.

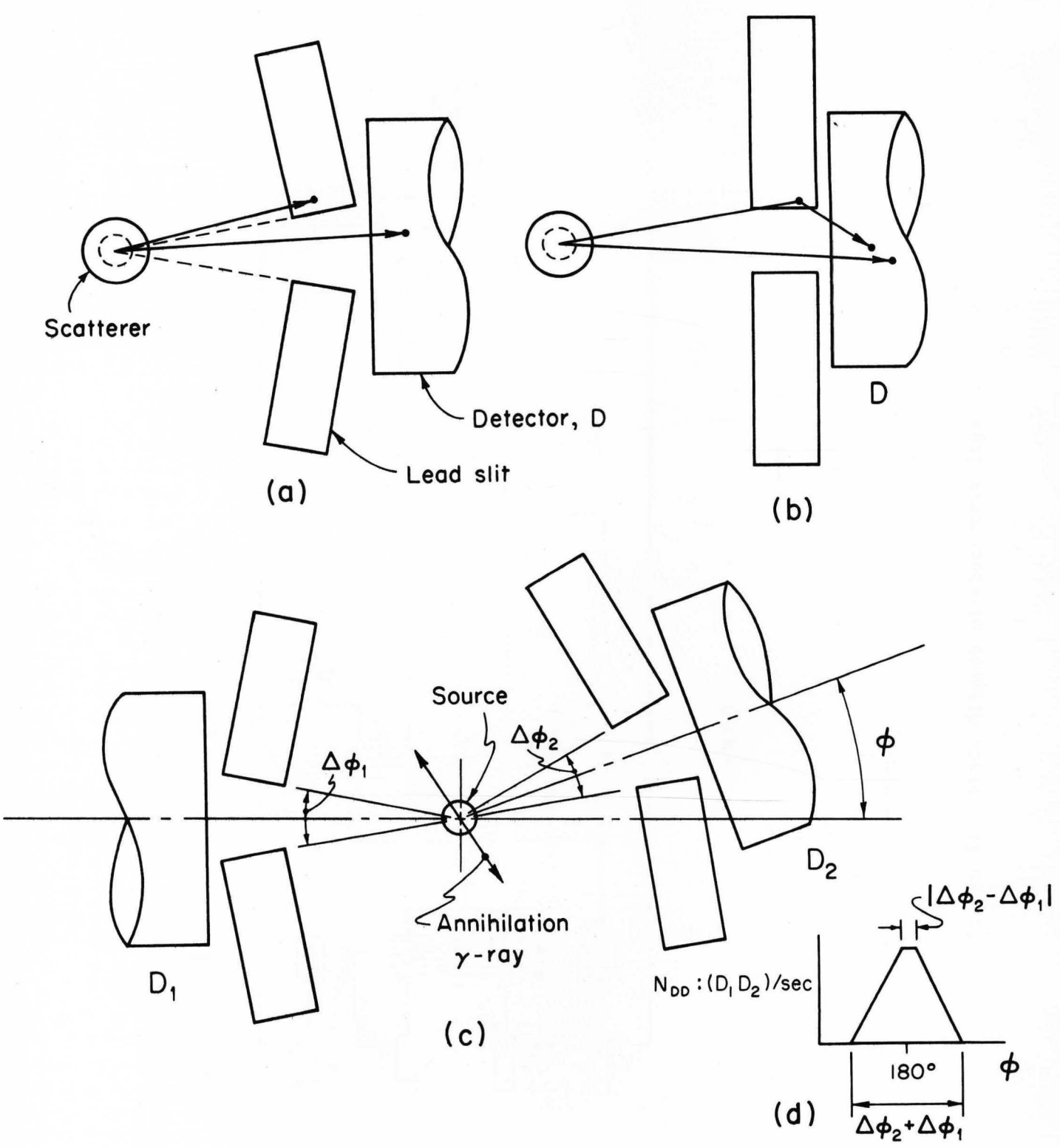

Figure 13. (a): Detector and azimuthal angles defining lead slit; this design reduces the probability for events shown in the rejected design, (b). Tha angular acceptance of the slits was measured as in (c), using the plot of D_1D_2 coincidences, (d).

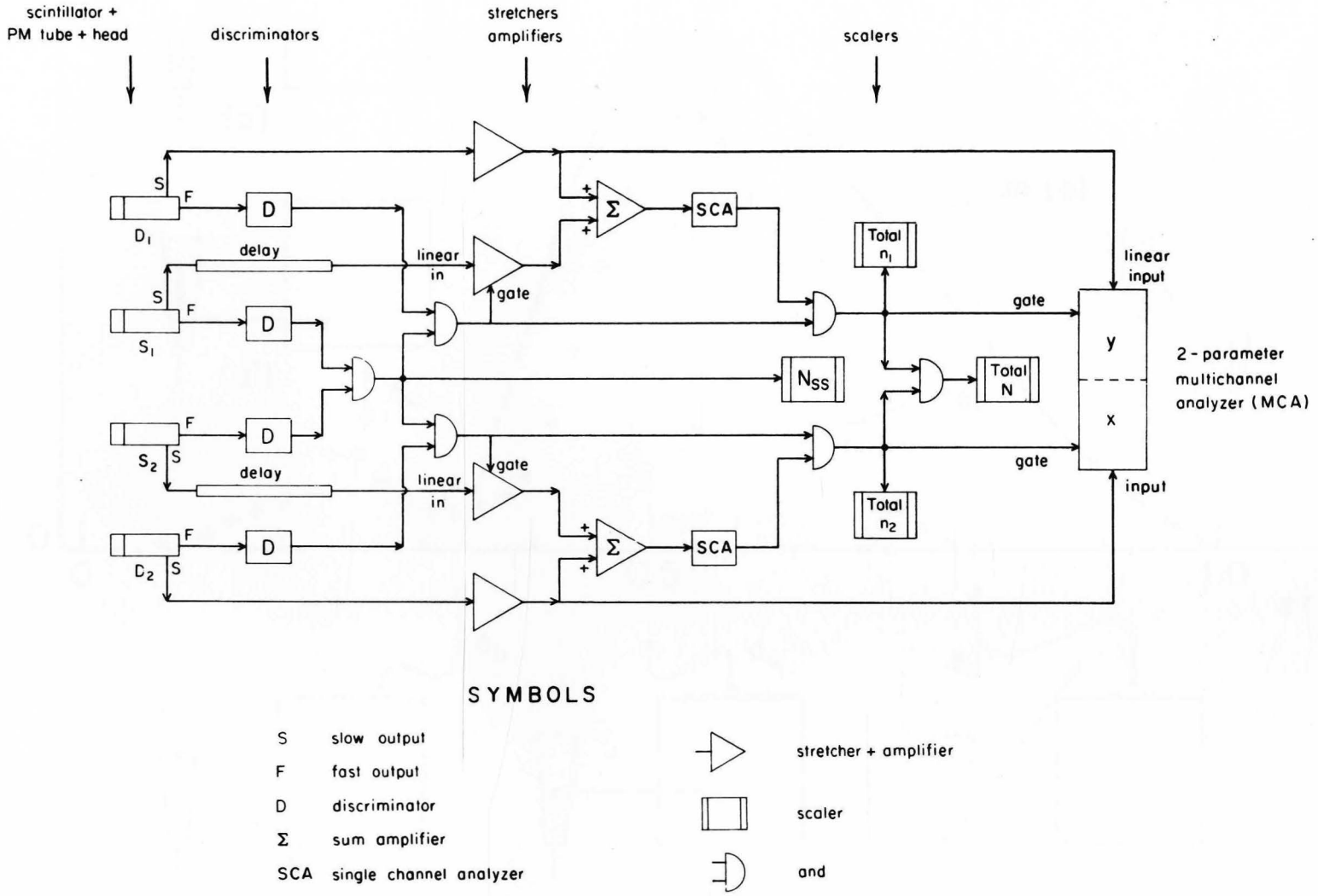

Figure 14. Block diagram of electronic logic.

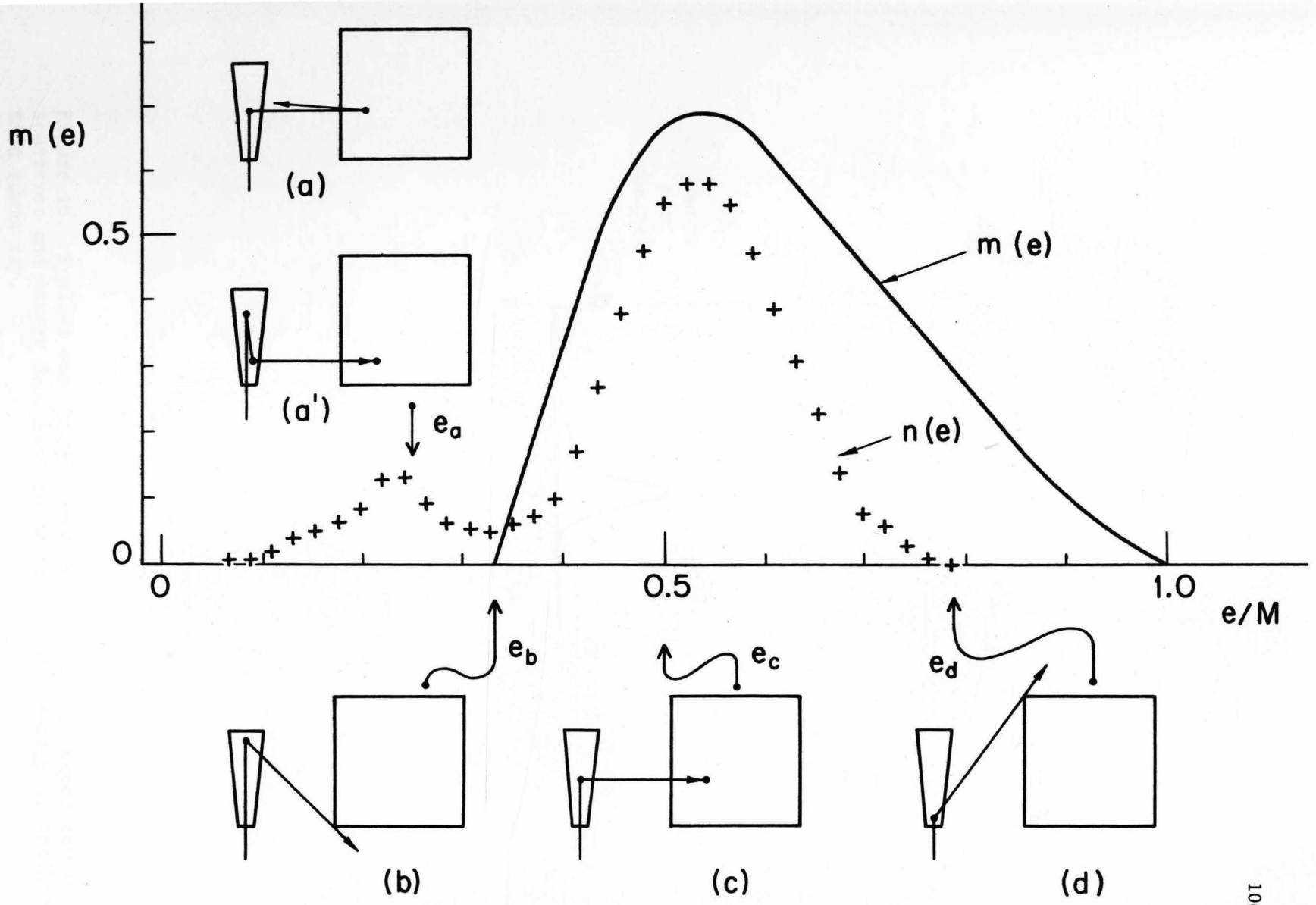

Figure 15. Spectrum of three-fold "n_1" coincidence events n(e) and typical events contributing to various parts of the spectrum. The amplitude of the cos 2ϕ dependence of R is proportional to the theoretical function m(e) shown as a solid line.

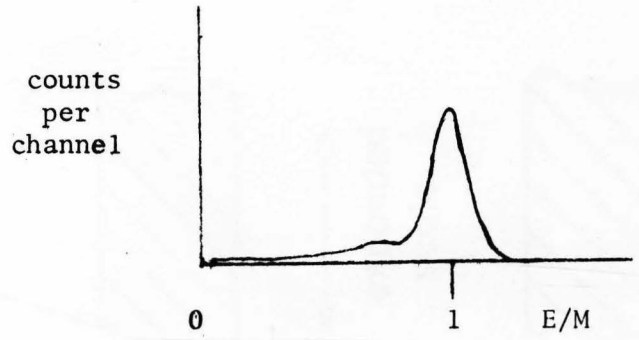

Figure 16. Typical sum energy spectrum. E = energy deposited in scatterer and energy deposited in detector. M = energy of annihilation gamma ray.

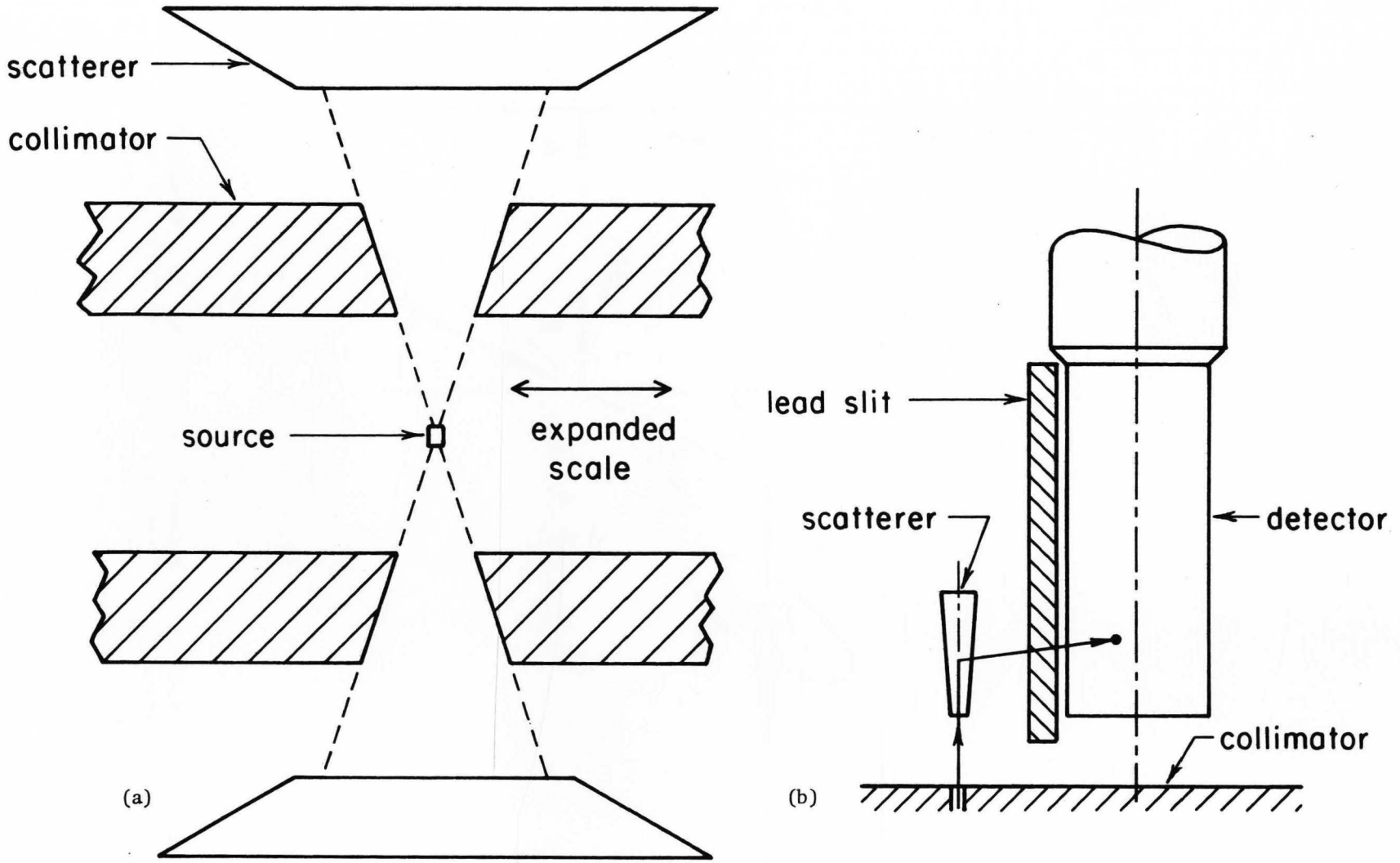

Figure 17. Modifications which would result in greater accuracy:
(a) A small diameter source and a conical collimator hole make a well defined beam, with a diameter smaller than the diameter of the scatterer.
(b) A long detector would enable a wider range of scattering angles to be accepted.

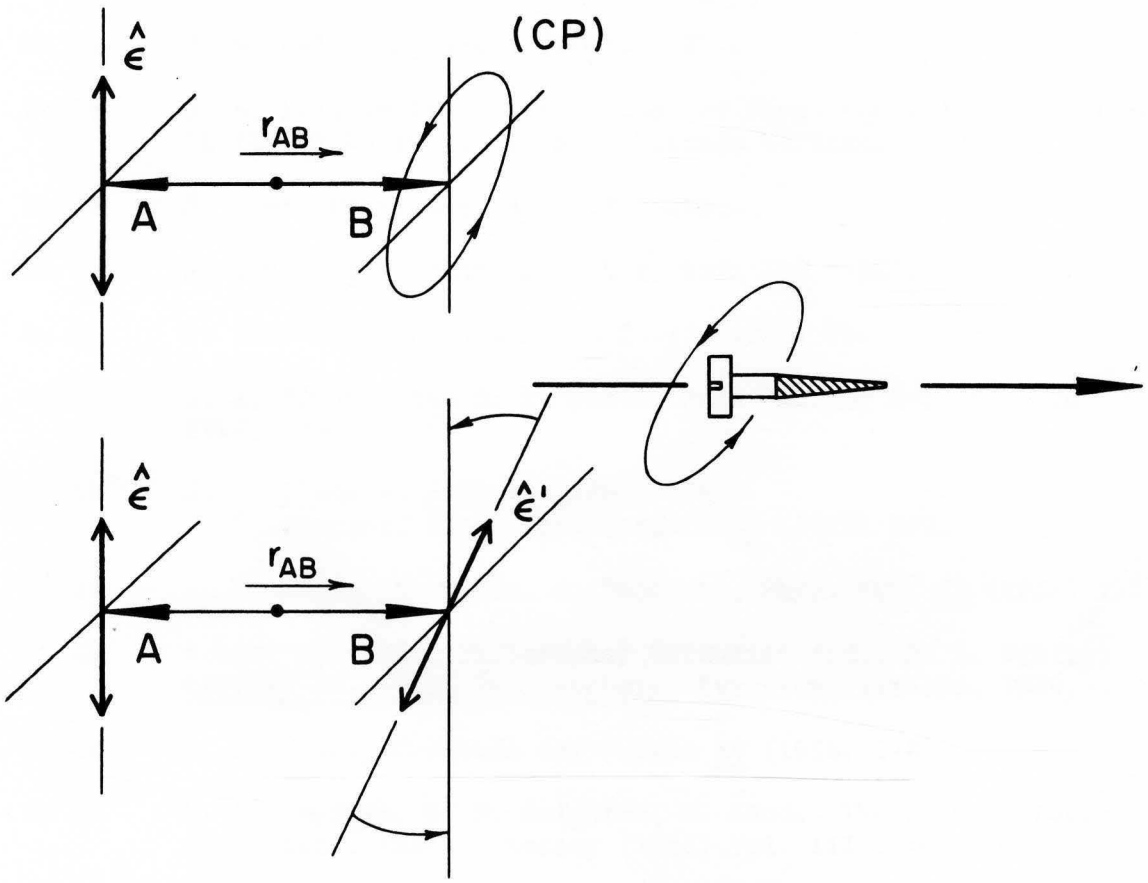

Figure 18. If the linear polarization of one photon, $\hat{\varepsilon}$, is determined, then conservation of parity requires that the other photon has linear polarization, $\hat{\varepsilon}'$ and not circular polarization. Furthermore, $\hat{\varepsilon}' \perp \hat{\varepsilon}$ or $\hat{\varepsilon}' \parallel \hat{\varepsilon}$. Otherwise a right-handed screw may be defined as shown.

REFERENCES

Ba 71 G. Bacci et. al., Lett. Nuovo Cim. 2 (1971) 73.

Bal 71 V. E. Balakin et al., Phys. Letters 34B (1971) 99.

Be 55 G. Bertolini et al., Nuovo Cim. 2 (1955) 661.

Be 64 J. S. Bell, Physics 1 (1964) 195.

Be 70 J. S. Bell in Proc. Int. School of Phys. "Enrico Fermi", Course IL (1970) Varenna. To be published by Academic Press.

Bo 35 N. Bohr, Phys. Rev. 48 (1935) 696.

Bo 57 D. Bohm and Y. Aharonov, Phys. Rev. 108 (1957) 1070.

Bo 60 D. Bohm and Y. Aharonov, N.C. 17 (1960) 964.

Br 70 S. J. Brodsky and S. D. Drell, Ann. Rev. of Nuc. Sci. 20 (1970) 147.

Cl 69 J. F. Clauser, BAPS 14 (1969) 578.
J. F. Clauser, Phys. Rev. Letters 23 (1969) 880.

Ei 35 A. Einstein, N. Rosen, B. Podolsky, Phys. Rev. 47 (1935) 777.

Ei 49 Albert Einstein, Philosopher Scientist (ed., P. A. Schlip) Library of Living Philosophers, Evanston Illinois, 1949.

Ev 58 R. D. Evans, Handbuch der Physik 34 (1958) 218.

Fe 65 R. P. Feynman, R. B. Leighton, M. Sands, The Feynman Lectures in Physics, Addison Wesley (1965) Vol. III., sec. 18-5.

Fr 70 R. Friedberg, private communication.

Fu 36 W. H. Furry, Phys. Rev. 49 (1936) 393 and 476.

Ho 52 J. I. Hoover, W. R. Faust, C. F. Dohne Phys. Rev. 85 (1952) 58.

Ho 69 M. Horne, Thesis, Boston University, 1969

In 61 D. R. Inglis, Rev. Mod. Phys. 33 (1961) 1.

Ja 70 J. M. Jauch in Proc. Int. School of Phys. "Enrico Fermi", Course IL (1970) Varenna. To be published by Academic Press.

Ka 70a L. Kasday in Proc. Int. School of Phys. "Enrico Fermi" Course IL (1970) Varenna. To be published by Academic Press.

Ka 70b L. Kasday, J. Ullman and C. S. Wu, BAPS 15 (1970) 586.

Ko 67 C. A. Kocher and E. D. Commins, Phys. Rev. Letters 18 (1967) 575.

Kl 29 O. Klein and Y. Nishina, Z. Phys. 52 (1929) 853.

Ku 67 O. F. Kulikov et al., Prib. Tekh Eksp. 4 (1967) 14. Translated in Instr. Exp. Meth. (USA) 4 (1967) 710.

La 60 H. Langhoff, Z. der Phys. 160 (1960) 186.

Le 67 C. M. Lederer et al., Table of Isotopes, Wiley, New York, 1967.

Mu 64 H. Müller, Congres International de Physique Nucleaire (Paris: Centre National de la Recherche Scientifique, Vol 2 (1964) 154.

Me 50 F. Metzger and M. Deutsch, Phys. Rev. 78 (1950) 551.

Pe 60 A. Peres and P. Singer, N.C. 15 (1960) 907.

Pr 47 M. H. L. Pryce and J. C. Ward, Nature 160 (1947) 435.

Ra 68 A. S. Raju et al., J. Phys. A. 1 (1968) 251.

Re 68 M. Renniger, private communication, 1968.

Sa 69 J. R. Sauer, IEEE Trans. Nuc. Sci. NS-16 (1969) 1069.

Sh 70 A. Shimony in Proc. Int. School of Phys. "Enrico Fermi" Course IL (1970) Varenna. To be published by Academic Press.

Si 65 M. Singh et al., Nuc. Phys. 62 (1965) 267.

Si 69 C. K. Sinclair et al., IEEE Trans. Nuc. Sci. NS-16 (1969) 1065.

Sn 48 H. S. Snyder et al., Phys. Rev. 73 (1948) 440.

We 46 A. Wheeler, Ann. New York Academy of Sciences 48 (1946) 219.

Wu 50 C. S. Wu and I. Shaknov, Phys. Rev. 77 (1950) 136.
Earlier measurements were made by:
E. Bleuler, H. L. Bradt, Phys. Rev. 73 (1948) 1398.
R. C. Hanna, Nature 162 (1948) 332.
H. S. Snyder et al., (ibid.)

Ya 50 C. N. Yang, Phys. Rev. 77 (1950) 242.